V. Artero, M. Fontecave, and M. Chavarot-Kerlidou

DOI: 10.1002/anie.201007987

Photocatalytic Water Splitting

Splitting Water with Cobalt

Vincent Artero, Murielle Chavarot-Kerlidou, and Marc Fontecave**

Keywords:
bioinorganic chemistry · electrocatalysis · hydrogen production · photocatalysis · water oxidation

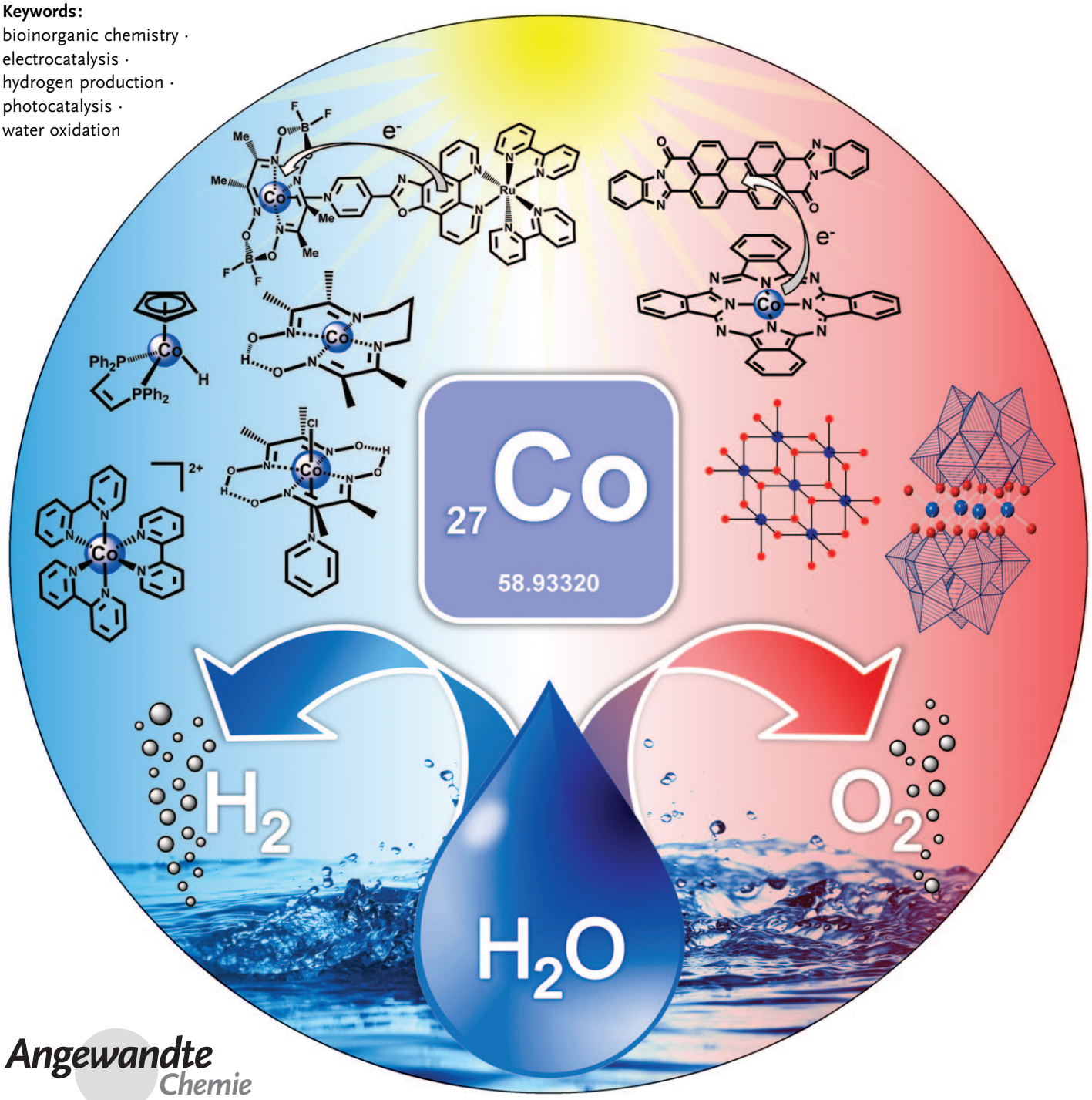

The future of energy supply depends on innovative breakthroughs regarding the design of cheap, sustainable, and efficient systems for the conversion and storage of renewable energy sources, such as solar energy. The production of hydrogen, a fuel with remarkable properties, through sunlight-driven water splitting appears to be a promising and appealing solution. While the active sites of enzymes involved in the overall water-splitting process in natural systems, namely hydrogenases and photosystem II, use iron, nickel, and manganese ions, cobalt has emerged in the past five years as the most versatile non-noble metal for the development of synthetic H_2- and O_2-evolving catalysts. Such catalysts can be further coupled with photosensitizers to generate photocatalytic systems for light-induced hydrogen evolution from water.

From the Contents

1. Introduction

Few biological processes have attracted the interest from bioinorganic chemists as photosynthesis. Photosynthesis allows bacteria, algae, and plants to use solar energy to sustain their growth through the production of biomass. From its origin, mankind has used this biomass, such as wood, as its main energy resource. Fossil fuels now form the basis of the world economy. As their reserves are rapidly diminishing, the current trend is to develop processes to transform biomass into biofuels, but this is likely to compete with agricultural food production. At the same time, photovoltaics appears to be one of the most promising energy technologies as it allows the conversion of solar energy into electrical power. Actually, the amount of solar energy reaching planet Earth is several orders of magnitude greater than that required for human development, so that even low conversion efficiency would be sufficient to solve the upcoming energy crisis.[1] The issue here is to find a way to store this energy, because worldwide energy demand does not correlate with the availability of sunlight.[2] Hydrogen production, through the reduction of water in electrolysers, is currently one of the most convenient ways to store energy durably if the electrical energy is initially obtained from renewable resources. While electrolysis is a mature and robust technology, the most promising devices, which are based on proton exchange membranes, rely on the use of platinum as an electrocatalyst to accelerate both hydrogen evolution [Eq. (1)] and water oxidation [Eq. (2)].

$$2\,H^+ + 2\,e^- \rightarrow H_2 \quad (1)$$

$$H_2O \rightarrow {}^1\!/_2\,O_2 + 2\,H^+ + 2\,e^- \quad (2)$$

However, this rare and expensive metal is not itself a sustainable resource,[3] so the viability of a hydrogen economy depends on the design of new efficient and robust electrocatalytic materials based on abundant elements. The question of the limitations of resources of chemical elements on earth and of the new strategies to develop to allow a sustainable access to them is in fact a very general one. It not only applies to noble metals but also to lithium and rare-earth elements, for example. It will undoubtedly result in the emergence of a new scientific field of research which will address the three following issues: 1) Reducing the amounts of active materials in technological devices; 2) substituting cheap and abundant elements for expensive and rare ones; and 3) developing technologies to recover and recycle all of these elements.

Another issue involves using sunlight directly as the energy source for water splitting, without the intermediate production of electricity, thereby reproducing the direct light-to-chemical energy transduction achieved by photosynthetic organisms. In such a process, light is used to extract electrons from water, which is oxidized to O_2.[4] Most organisms use these photogenerated electrons to reduce atmospheric carbon dioxide and produce carbohydrates, proteins, or lipids as the main constituents of their biomass, but some microorganisms, such as cyanobacteria or microalgae, are able, under very specific conditions, to photosynthesize hydrogen as well.[5–8] Understanding this biological process and exploiting this knowledge for designing original synthetic molecular systems achieving a similar function is the basis of a large field of research called "artificial photosynthesis".[9–11] When restricted to hydrogen production from sunlight and water, it falls into the category of light-driven water splitting [Eq. (3)]. This reaction is thermodynamically uphill, with

$$H_2O \rightarrow H_2 + {}^1\!/_2\,O_2 \quad (3)$$

2.46 eV ($\Delta_r G^\circ = 238\ kJ\,mol^{-1}$) required to split one water

[*] Dr. V. Artero, Dr. M. Chavarot-Kerlidou, Prof. M. Fontecave
Laboratoire de Chimie et Biologie des Métaux
Université Joseph Fourier, Grenoble
CNRS, UMR 5249, CEA, DSV/iRTSV/LCBM, CEA-Grenoble, Bat K'
17 rue des Martyrs, 38054 Grenoble cedex 9 (France)
Fax: (+33) 4-3878-9124
E-mail: vincent.artero@cea.fr
Prof. M. Fontecave
Collège de France
11 place Marcellin-Berthelot, 75005 Paris (France)
E-mail: marc.fontecave@cea.fr

molecule into H_2 and O_2. The energy of two photons from the visible (800 nm/1.56 eV–400 nm/3.12 eV) to infrared (down to 1014 nm/1.23 eV) domain is enough to drive this reaction to completion. Through this photochemical process, sun energy is thus stored and converted into H_2, which upon oxidation can release 2.46 eV per molecule back.

The whole natural process may be divided into three distinct steps: 1) an initial light-harvesting process and local charge separation at chlorophylls in photosystems I and II, 2) proton-coupled electron transfers between redox cofactors along the photosynthetic chain allowing further spatial charge separation and preventing charge recombination, and 3) multi-electron generation of hydrogen and oxygen catalyzed by remarkable enzymatic sites, such as the dinuclear NiFe and FeFe clusters in hydrogenases[12] or the oxygen-evolving $CaMn_4$ center (OEC) of photosystem II (PSII).[4]

While the first two topics have been the core of artificial photosynthesis for the last two decades, and also the subject of comprehensive reviews,[13–23] significant achievements have been made only in the recent years as far as the design of efficient molecular catalysts for both hydrogen and oxygen evolution is concerned. These comprise FeFe,[24] NiRu,[25–30] NiMn,[31] and NiFe[25,32–34] models of the active sites of hydrogenases as well as manganese[35] and ruthenium[36–40] catalysts as functional mimics of the PSII OEC. These systems have been reviewed recently.[24,25,41–44]

Although cobalt has no biological relevance for water splitting, and although it is significantly less abundant (20–30 ppm) than Fe (6.3 %), Mn (0.1 %), or Ni (90 ppm), it is now emerging as an interesting metal for its catalytic power for Reactions (1) and (2). In this Review, we discuss recent developments regarding the design, characterization, and evaluation of cobalt-based molecular catalysts and show how they can be coupled with photosensitizers to generate light-driven systems for H_2 or O_2 evolution. We also provide general methods to evaluate the performances of such molecular catalysts and show how such systems can be immobilized onto conducting materials so as to form electrodes or photoelectrodes to be integrated in a photoelectrochemical (PEC) cell for light-driven hydrogen generation from water. Finally we also discuss cobalt oxide materials, which appear to be promising catalysts for water oxidation.

2. Cobalt Catalysts for H_2 Evolution

Reduction of protons to hydrogen [Eq. (1)] appears to be a very simple reaction. Unfortunately it is slow on most electrodes, except on platinum and other noble metals, because it is a multielectron process. The combination of a standard and cheap electrode material with a coordination complex that is able to catalyze the reaction at a reasonable potential so as to lower the activation potential is a relevant strategy as an alternative to the use of platinum.[45]

The potential of H_2-evolving cobalt-based catalysts has recognized a long time ago.[46] Most of the catalytically active systems are square-planar macrocyclic or pseudo macrocyclic complexes, such as [14]diene-N_4 macrocyclic cobalt complexes **1** and **2**[47] and [14]tetraene-N_4 analogues **3**–**5**[48] (Figure 1). Water-soluble cobalt porphyrin derivatives **6**–**8** (Figure 2),[49] are also quite stable as catalysts but are prone to adsorb at the electrode surface. The cobaloxime [Co-$(dmgBF_2)_2(OH_2)_2$] (**9**; Figure 3), initially developed as a mimic of vitamin B_{12}, was also recognized early on as a

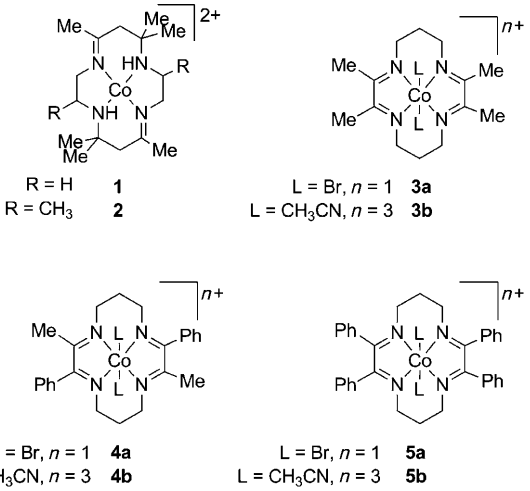

Figure 1. Structures of cobalt complexes with [14]tetraene-N_4 and [14]diene-N_4 ligands.

Vincent Artero received his PhD in 2000 from the University Pierre et Marie Curie (Paris 6) under the supervision of Prof. A. Proust on organometallic derivatives of polyoxometalates. After a postdoctoral stay in Aachen with Prof. U. Kölle, he joined the Laboratory of Chemistry and Biology of Metals in Grenoble in 2001, where he obtained a position in the Life Science Division of the CEA. His current research interests are in the structural and functional hydrogenase models for the design of artificial systems for the photo- and electrochemical production of hydrogen.

Murielle Chavarot-Kerlidou received her PhD in 1998 from the University Joseph Fourier (Grenoble). After a postdoctoral period in the group of Dr. Zoe Pikramenou (University of Birmingham, UK) studying photoinduced supramolecular processes based on luminescent metallocyclodextrins, she spent two years in the group of Marc Fontecave developing chiral-at-metal ruthenium catalysts for enantioselective oxidation. She obtained a CNRS position in 2002 at the Université Pierre et Marie Curie (Paris), where her research interests dealt with the development of new applications of the arene–tricarbonyl metal complexes. In 2009, she moved to the Laboratory of Chemistry and Biology of Metals to work on hydrogen photoproduction.

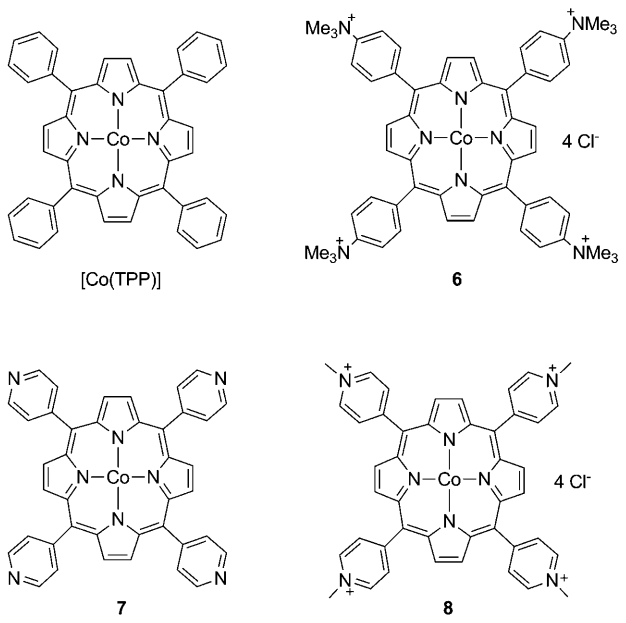

Figure 2. Structures of cobalt porphyrin complexes.

powerful catalyst for hydrogen evolution from an acidic aqueous solution in the presence of reducing agents such as divalent metal salts.[50] Recently, **9** and other cobaloxime derivatives **10**–**14a** (Figure 3) were shown to act as electrocatalysts for H_2 evolution from nonaqueous acidic solutions, with the electrons provided by a glassy carbon working electrode.[48,51–54] Even more recently, imine/oxime cobalt complexes **15**–**21** (Figure 4) were also investigated.[55,56] Compounds **15**–**17**, which contain tetradentate ligands, are much more stable with respect to hydrolysis than cobaloxime.[55] These systems all have the open axial coordination sites required for catalysis. Octahedral polypyridine derivatives, such as **22** derived from $[Co(bipy)_3]^{2+}$ or **23** (Figure 5) with two labile ligands in *cis* positions, have been reported.[57–61] Some coordinatively saturated compounds, such as octahedral hexaamino complexes **24**–**27** (Figure 6),[62] and including sepulchrate derivatives[62,63] and clathrochelate trisdioxime compounds **28**–**29** (Figure 7),[64]

Marc Fontecave is a member of the French Academy of Sciences and has been Professor of Chemistry of Biological Processes at the Collège de France in Paris since 2008. He spent 20 years as Professor of the Université Joseph Fourier in Grenoble, after a PhD at the Ecole Normale Supérieure in Paris and postdoctoral research at the Karolinska Institute in Stockholm. He is currently the President of the Scientific Council of the City of Paris. His research group studies the structural and functional properties of metal-containing biological redox systems, in particular iron–sulfur enzymes involved in a variety of metabolic and biosynthetic processes. He has developed bioinspired chemical approaches to obtain original molecular catalysts, for example, for hydrogen production.

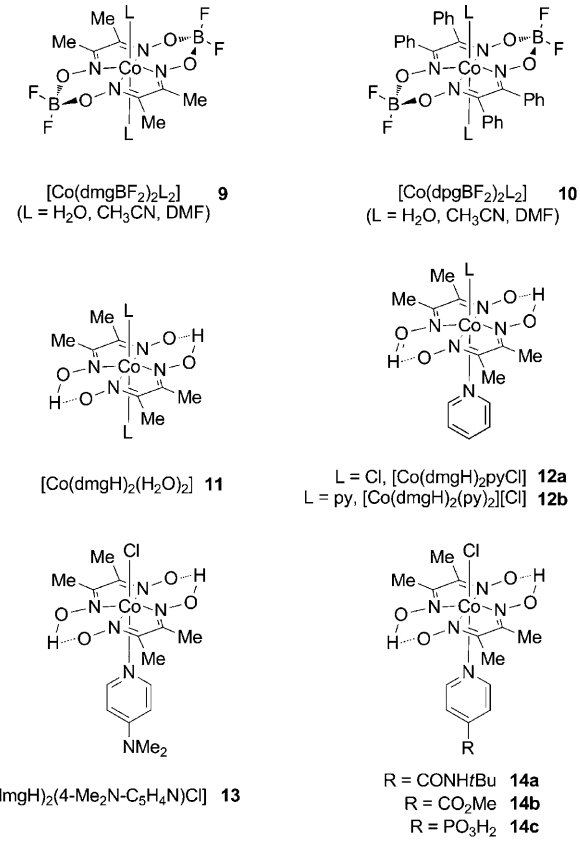

Figure 3. Structures of cobaloximes.

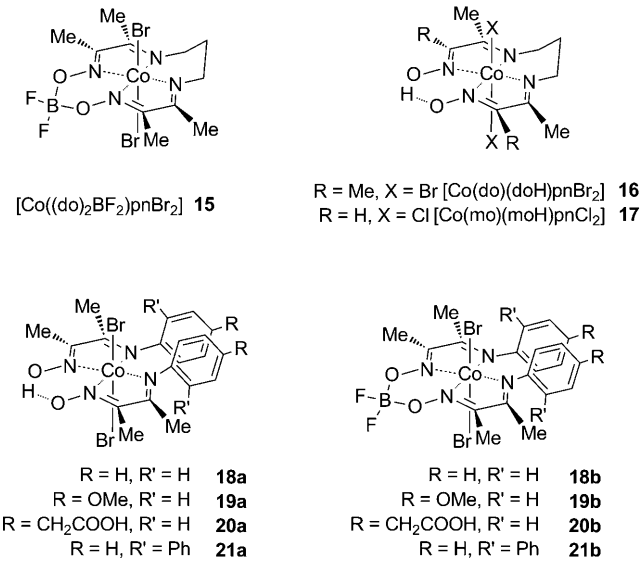

Figure 4. Structures of diimine-dioxime cobalt compounds.

have also been described. A last class is provided by organometallic compounds containing cyclopentadienyl (**30**–**33**)[63,65,66] or diphosphine (**34**)[67,68] ligands (Figure 8). We will not survey all of the examples, but will rather select some of the above-mentioned systems to highlight the specific features that are key to provide catalytic H_2-evolving activity.

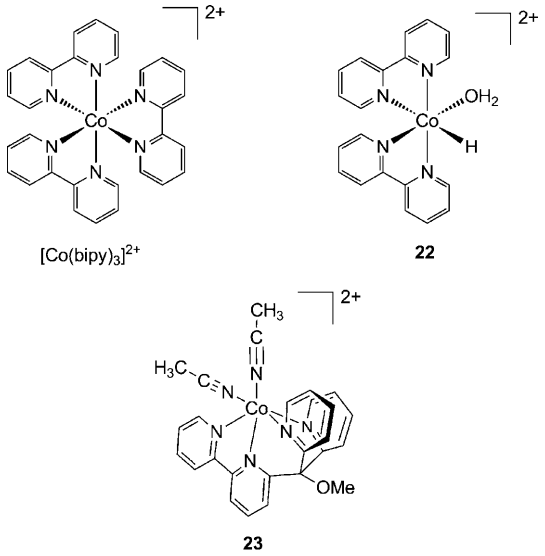

Figure 5. Structures of cobalt polypyridine compounds

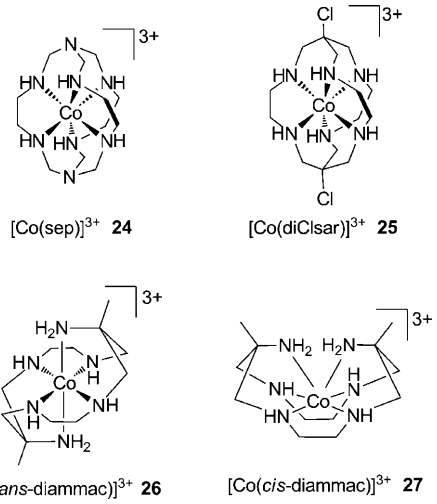

Figure 6. Structures of hexaaminocobalt complexes

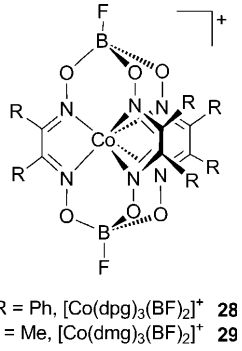

Figure 7. Structures of clathrochelate tris(dioxime) cobalt compounds.

2.1. Evaluation of the H_2-Evolution Catalysts

Molecular electrocatalysts are currently evaluated in organic or aqueous solution. The common way to demonstrate electrocatalytic ability for hydrogen evolution consists

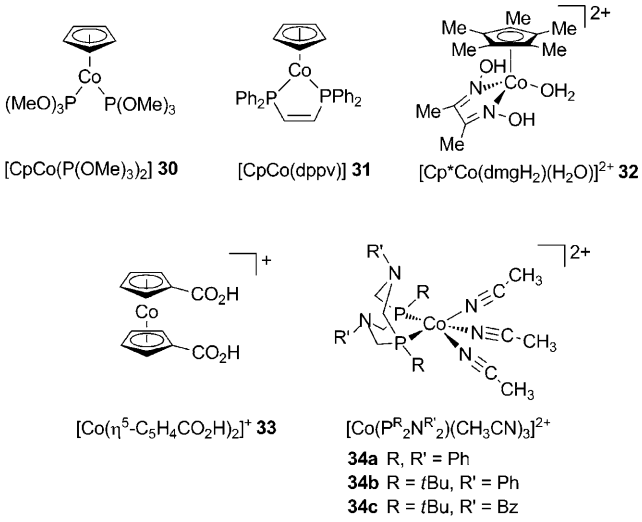

Figure 8. Structures of organometallic cobalt catalysts (Bz = benzyl).

in recording cyclic voltammograms (CV) of the studied complex in a given solvent in the presence of increasing amounts of a proton source, typically a weak acid. Carbon, gold, or ITO (indium tin oxide) are typically used as electrode materials for such studies. Catalytic hydrogen evolution is evidenced by the appearance of an irreversible wave that grows larger with increasing acid concentrations. Analytical confirmation of H_2 production is generally carried out with a bulk electrolysis experiment coupled to coulometric monitoring on a solution containing the catalyst and a large excess of acid. The electrode potential is kept constant at a value corresponding to that of the electrocatalytic wave. The evolved hydrogen is characterized by gas chromatography (GC) and quantified either by GC or volumetric measurements. Bulk electrolysis experiments can also help provide evidence for catalytic activity, which is too slow to observe at the CV scan rate.

Figure 9 shows the cyclic voltammograms of the cobaloxime $[Co(dmgH)_2pyCl]$ (**12a**) recorded in DMF at a glassy

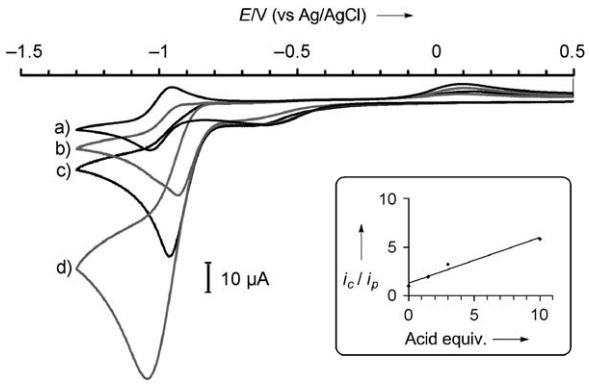

Figure 9. Cyclic voltammograms of **12a** (1.0 mmol L^{-1}) in the presence of various amounts of Et_3NHCl recorded in a DMF solution of nBu_4NBF_4 (0.1 mol L^{-1}) on a glassy carbon electrode at 100 mV s^{-1}: a) 0 equiv, b) 1.5 equiv, c) 3.0 equiv, d) 10 equiv. Potentials are quoted versus Ag/AgCl/NaCl 3 mol L^{-1}. Inset: catalytic current enhancement versus acid concentration.

carbon electrode in the presence of increasing amounts of triethylammonium chloride.[51] The first catalytic parameter that can be extracted from these data is the potential at which the reduction of Et_3NH^+ into H_2 occurs. However, depending on the authors, it is defined either as the position of the peak of the catalytic wave, that of the onset of the same wave, or that for which half of the maximum current is obtained (half-wave potential). In practice, this leads to differences of up to 200 mV in the measured values for the same catalyst assayed under similar conditions. Furthermore, distinct electrocatalysts are generally assayed under different conditions (choice of solvent, proton source, acid concentration, temperature) and the standard potential of the H^+/H_2 couple strongly depends on both the solvent and the pK_a value of the acid used as a source of protons. Therefore, a direct comparison of different catalysts exclusively on the basis of the electrocatalytic potential reported for hydrogen evolution is often impossible. This problem can be overcome if the overpotential requirement is instead considered for comparison. This parameter is defined as the difference between the potential needed to be applied to the system to make it function at a specified rate and the standard potential of the redox couple of the H^+/H_2 couple under the operating conditions.[72] It is a measure of the energy required for driving this reaction at a significant rate as compared to the thermodynamic limit[72–74] and is related to an activation energy, as temperature does for homogeneous reactions. It thus corresponds to a fraction of energy that is lost during the reaction and directly relates to the efficiency of the energetic transduction process. We recently proposed a standardized method using the half-wave potential value of the electrocatalytic wave as a reliable determination of the overpotential requirement for a given catalyst. This new method enables direct comparison between systems assayed under various conditions and over a wide range of concentrations of the acid, and we hope that it will be used for the characterization of the new catalytic systems to be reported.[72,75] In the following, however, we will exclusively quote the overpotential requirement values found in the original reports. For the system reported in Figure 9, electrocatalytic hydrogen evolution occurs at a potential of −0.98 V vs Ag/AgCl, which corresponds to an overpotential requirement of about 200 mV. Overpotential requirement values in the 200–300 mV range are obtained with other cobaloxime derivatives **9**–**14** and diimine-dioxime cobalt complexes **15**–**21**, which appear on this basis to be the most efficient H_2-evolving cobalt catalysts to date.

The second parameter used to characterize a catalyst is the turnover frequency (TOF). As the current measured at an electrode is correlated to the number of electrons exchanged per second with the redox-active compounds in the solution (here the catalyst), there is a direct relationship between turnover frequency and the catalytic current measured by cyclic voltametry. The turnover frequency (apparent first-order rate constant) can however be determined analytically in only very specific cases depending on the catalytic regime.[53,67,76] Numeric simulations of the cyclic voltammograms using DigiSim, DigiElch,[77–82] or related software may allow an estimation of the catalytic rate, but only if the catalytic mechanism is established.[48,51,52] As an example, the rate-determining step in H_2 evolution catalyzed by **12** (Figure 9) is the protonation of a metal–hydride complex, and its constant was estimated to $1.35 \times 10^4\ mol^{-1}\,L\,s^{-1}$. This yields a turnover frequency of $1350\ s^{-1}$ for an acid concentration of $0.1\ mmol\,L^{-1}$.

Alternatively, the catalytic current-enhancement parameter, expressed as the i_c/i_p ratio with i_c being the catalytic current and i_p the peak current associated with a monoelectronic wave of the catalyst, is used as a proxy for the turnover frequency. The inset in Figure 9 shows that the catalytic current enhancement depends linearly on the acid concentration for low concentrations of the proton source, which means that the catalytic rate is limited by mass transport.[83] Although the catalytic current enhancement does not allow an accurate estimation of the turnover frequency, this parameter allows catalysts to be compared under similar acid concentrations without any knowledge of their respective operating mechanisms. It is important to note that the rate of electrolysis cannot be related to the intrinsic turnover frequency of the catalyst, as in such an experiment the current is limited by diffusion within the separated compartments of the electrolysis cell.

Finally, a catalyst suitable for practical applications needs to have relatively high thermodynamic and kinetic stability under operating conditions and thus high turnover numbers. From the amount of catalyst present in the cell and the charge passed through the cell during a bulk electrolysis experiment, a turnover number can be simply derived. The robustness is thus related to the total turnover number achieved by the catalyst before deactivation. Most of the time, bulk electrolysis experiments are not carried out until complete loss of activity; thus, a lower limit for stability can only be determined from the reported data.

Another useful parameter for characterizing the system is the Faradaic yield, which is also measured during a bulk electrolysis experiment and corresponds to the ratio of the amount of H_2 evolved divided by half of the charge (expressed in Faraday units) passed through the cell. The Faradaic yield quantifies the selectivity of the catalyst for H_2 evolution; values far from unity indicate that a significant amount of charge is used to produce something apart from H_2. Low turnover numbers together with low Faradaic yields are associated with extended reductive decomposition of the catalyst. Table 1 gathers the performance of the various cobalt-based catalysts shown in Figure 1–8.

Typically, molecular catalysts do not have turnover numbers of more than a few hundred. This figure may appear quite low when put in perspective of technological applications. However, these are only preliminary characterizations, and exploitation of a molecular catalyst in a practical device can only be achieved after heterogenization; that is, incorporation into an electrode material. In this configuration, more extensive stability tests have then to be carried out. It is interesting to note that grafting of such molecular catalysts onto the surface of an electrode material can provide stabilizing interactions and avoid bimolecular degradation upon cycling, thus allowing a significant increase of the robustness of the catalyst.[84,85]

Table 1: Electrocatalytic performances of the distinct cobalt-based H_2-evolving systems described in the literature.

		Conditions		CV	Bulk electrolysis experiments			
Catalyst	Electrode	Proton source	Medium	Electrocatalytic potential	Applied potential	TON (reaction time)	Faradaic yield	Ref.
1	Hg[b]	H_2O	0.1 mol L^{-1} KNO_3 in H_2O/CH_3CN 2:1 (v/v) or H_2O only		−1.6 V (SCE)	140 (18 h)	80%	[47]
2	Hg[b]	H_2O	0.1 mol L^{-1} KNO_3 in H2O/CH_3CN 2:1 (v/v) or H_2O only		−1.5 V (SCE)	164 (18 h)	80%	[47]
3a/3b	GCE[a]	$TsOH·H_2O$	CH_3CN	−0.35– −0.38 V (SCE)	−0.58 V (SCE)	5 (30 min)	90–100%	[48]
4a/4b	GCE[a]	$HBF_4·Et_2O$	CH_3CN	−0.20– −0.25 V (SCE)	−0.48 (SCE)	ca. 2 (30 min)	20–25%	[48]
6, **7**, **8**	Hg[b]	Aqueous CF_3COOH (0.1 mol L^{-1})			−0.95 V (SCE)	0.65 (20 min)	>90%	[49]
9 (L = H_2O)	Graphite	Et_3NHBF_4 (0.2 mol L^{-1})	1,2-$C_2H_4Cl_2$		−0.90 V (Ag/AgCl)	80 (17 h)	>85%	[51]
9 (L = CH_3CN)	Hg[b]	*p*-cyanoanilinium (0.1 mol L^{-1})	CH_3CN	−0.34 V (Ag/AgCl), GCE[a]	−0.5 V (Ag/AgCl)	46 (30 min)		[52]
9 (L = CH_3CN)	Hg[b]	CF_3COOH (0.1 mol L^{-1})	CH_3CN	−0.43 V (Ag/AgCl), GCE[a]	−1.0 V (Ag/AgCl)	15 (1 h)		[52]
		CF_3COOH (0.1 mol L^{-1})	CH_3CN		−0.5 V (Ag/AgCl)	7 (1 h)		[52]
9 (L = CH_3CN)	Hg[b]	Et_3NHCl (0.1 mol L^{-1})	CH_3CN		−1.6 V (Ag/AgCl)	14 (1 h)		[52]
		Et_3NHCl (0.1 mol L^{-1})	CH_3CN		−1.0 V (Ag/AgCl)	3–4 (1 h)		[52]
9 (L = CH_3CN)	GCE[a]	CF_3COOH (0.045 mol L^{-1})	CH_3CN	−0.55 V (SCE)	−0.72 V (SCE)	20 (1 h)	ca. 100%	[53]
10	GCE[a]	$HCl·Et_2O$ (7.5 mmol L^{-1})	CH_3CN	−0.28 V (SCE)	−0.37 V (SCE)	11 (1 h)	90%	[53]
12	Graphite	Et_3NHBF_4 (0.2 mol L^{-1})	1,2-$C_2H_4Cl_2$		−0.90 V (Ag/AgCl)	100 (2.5 h)	>85%	[51]
12–14	GCE[a]	Et_3NHCl	DMF	−0.98 V (Ag/AgCl)				[51]
15	Graphite	*p*-cyanoanilinium (0.3 mol L^{-1})	CH_3CN	−0.82 V (Fc^+/Fc)	−0.82 V (Fc^+/Fc)	20 (3 h)	100%	[55]
16	Graphite	*p*-cyanoanilinium (0.3 mol L^{-1})	CH_3CN	−0.78 V (Fc^+/Fc)	−0.78 V (Fc^+/Fc)	40 (3 h)	92%	[55]
18a	GCE[a]	$TsOH·H_2O$ (53 mmol L^{-1})	CH_3CN		−0.48 V (SCE)	ca. 4	ca. 10%	[56]
18b					−0.73 V (SCE)			[56]
19a					−0.75 V (SCE)	ca. 3	ca. 10%	[56]
19b					−0.70 V (SCE)	ca. 30	ca. 55%	[56]
20a					−0.52 V (SCE)	ca. 15	ca. 20%	[56]
20b					−0.68 V (SCE)	ca. 25	ca. 70%	[56]
21a					−0.66 V (SCE)	ca. 10	ca. 20%	[56]
21b					−0.58 V (SCE)	ca. 25	ca. 75%	[56]
23	GCE[a]	CF_3COOH	CH_3CN	−0.81 V (SCE)				[61]

Table 1: (Continued)

Catalyst	Conditions: Electrode	Conditions: Proton source	Conditions: Medium	CV: Electrocatalytic potential	Bulk electrolysis experiments: Applied potential	Bulk electrolysis experiments: TON (reaction time)	Bulk electrolysis experiments: Faradaic yield	Ref.
23	GCE[a]	CF_3COOH	0.1 mol L^{-1} KNO_3 in H_2O/CH_3CN 1:1 (v/v)	−1 V (SCE)				[61]
24	Hg[b]	Phthalate buffer pH 4	H_2O		−0.7 V (SCE)		55%	[63]
24, **26**, and **27**	Hg[b]	Phosphate buffer pH 7	H_2O		−1.0 V (Ag/AgCl)	1–2 (4 h)		[62]
27	Hg[c]	Aqueous $HClO_4$ solution pH 2		−1.3 V (Ag/AgCl)				[62]
28	Hg[b]	$HClO_4$ (33 mmol L^{-1})	CH_3CN	−0.4 V (SCE), GCE[a]	−0.55 V (SCE)	<0.5 (0.5 h)	10%	[64]
29	Hg[b]	$HClO_4$ (33 mmol L^{-1})	CH_3CN	−0.7 V (SCE), GCE[a]	−0.85 V (SCE)	ca. 1.5 (0.5 h)	35%	[64]
30	Hg[b]	pH 5	H_2O		−1.15 V (SCE)	20 (18 h)		[65]
33	Hg[b]	phosphate buffer pH 6.5	H_2O		−0.9 V (SCE)		42%	[63]
34	GCE[a]	HBF_4 or CF_3SO_3H	CH_3CN	−1.0 V (Fc^+/Fc)	−1.1 V (Fc^+/Fc)		100%	[67]
37	GCE[a]	2,6-dichloroanilinium tetrafluoroborate	CH_3CN	−0.3 V (SCE)				[69]
38	GCE[a]			−0.7 V (SCE)				[69]
[Co(TPP)]/Nafion	graphite[d]	pH 1 solution	H_2O		−0.7 V (Ag/AgCl)	70 h^{-1} (TOF)		[70]
[cobalt *meso*-tetrakis(2-aminophenyl)porphyrin]/poly(4-vinylpyridine-co-styrene)	graphite[d]	Phosphate buffer 0.1 mol L^{-1} pH 1.0	H_2O		−0.90 V (Ag/AgCl)	2×10^5 h^{-1} (TOF)		[71]

[a] Glassy carbon electrode. [b] Hg pool. [c] Hanging-drop Hg electrode. [d] Basal-plane pyrolytic graphite.

The rational improvements of catalytic performances can only be undertaken if the mechanism for H_2 evolution is clearly understood. The following sections address these issues.

2.2. Hydride Derivatives as Key Catalytic Intermediates

The mechanism of homogeneous hydrogen evolution catalyzed by cobalt complexes generally implies the formation of a cobalt(III) hydride species formed by protonation of a cobalt(I) intermediate. Such hydride derivatives have only been characterized for a few cobalt-based H_2-evolving catalysts.

Protonation of $[CpCo^I(P)_2]$ (P = PPh_3, PEt_3, or $P(OMe)_3$) and $[CpCo^I(P_2)]$ (P_2 = bis(diphenylphosphino)methane (dppm), 1,2-bis(diphenylphosphino)ethane (dppe), or *cis*-1,2-bis(diphenylphosphino)ethylene (dppv, such as in **31**)) by ammonium ions in organic solvents quantitatively yields the hydride derivatives $[CpCo^{III}H(P)_2]^+$ and $[CpCo^{III}H(P_2)]^+$, respectively, which have been characterized by ^1H NMR spectroscopy (Figure 10).[65]

Reduction of $[Co(dmgH)_2(PBu_3)Cl]$ (**35**) by $NaBH_4$ in a 50% (v/v) aqueous methanol solution buffered with sodium phosphate to pH ≈ 7 yields a precipitate of the blue complex

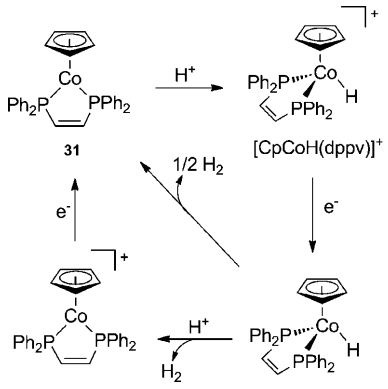

Figure 10. Preparation and reactivity of $[CpCoH(dppv)]^+$.

$[HCo(dmgH)_2(PBu_3)]$ (Figure 11).[86] The axial phosphine ligand stabilizes and thus inactivates the hydride species, resulting in a decrease of the H_2 evolution activity. The same synthetic procedure has been used for the preparation of hydride derivatives from the H-bridged or BF_2-annulated cobaloxime systems with an axial pyridine ligand.[86] A Co-H stretching band is observed at 2240 cm^{-1} in the IR spectrum; this band is observed at 1680 cm^{-1} for the deuteride analogue. The reported ^1H NMR chemical shift of the hydride ligand is $\delta = 6.0$ ppm, which is a surprising value for a formal hydride

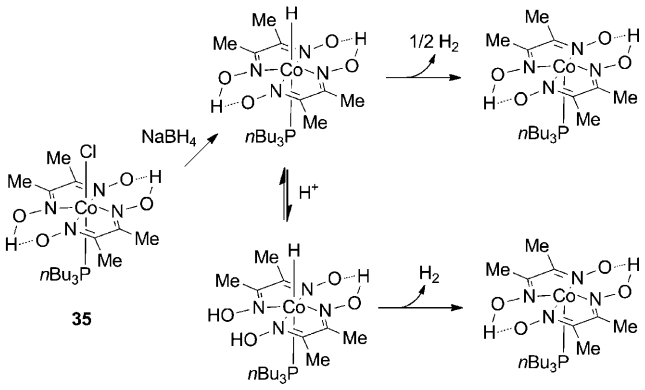

Figure 11. Reactivity of $[HCo(dmgH)_2(PBu_3)]$.

ligand but not unprecedented among transition metal hydrides[87–89] and in good agreement with a $Co^{\delta-}-H^{\delta+}$ polarization of the metal–hydrogen bond and the low basicity of the compound ($pK_a \approx 7$ in a water/ethanol mixture). As a consequence, UV/Vis spectra of Co^{III}–H species have the appearance of the Co^{I} compounds, with a large absorption band in the 550–650 nm region. $[HCo^{III}(dmgBF_2)_2]$, with no axial ligand or with a water molecule coordinated *trans* to the hydride, has been recently characterized in situ by Bakac and Szajna-Fuller; this species can be obtained by reduction either with $NaBH_4$ or with titanium(III) citrate in an aqueous buffer.[90]

Other hydride derivatives have been prepared or characterized in the course of pulse radiolysis experiments. These include studies with cobalt [14]diene-N_4 macrocyclic cobalt complexes, including **1**[91,92] and aqueous $CoSO_4$/2,2′-bipyridine mixtures, generating $[Co(bipy)_2(H_2O)H]^{2+}$ (**22**).[59]

In the case of the coordinatively saturated hexamine cobalt complexes **24**–**27** however, the formation of hydride intermediates has been definitively ruled out. Reduction to the Co^{I} state is in fact not possible[93] in this case because of geometric constraints within the encapsulating macrocycles.[94] The proposed mechanism[62] for H_2 evolution (Figure 12) thus involves the initial monoelectronic reduction of the Co^{III} complex, followed by elimination of a hydrogen atom ($H^{\bullet}$) from one amine group of the resulting adsorbed cobalt(II) species. Finally, two hydrogen atoms recombine at the surface of the electrode and generate H_2 while the complex is released in solution and protonated to regenerate the initial species.

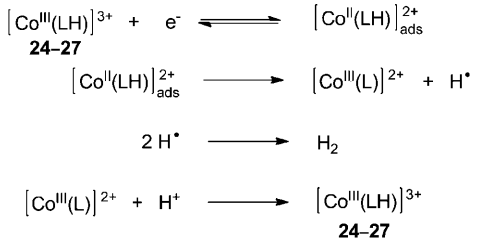

Figure 12. Mechanism for H_2 evolution catalysed by coordinatively saturated hexamine cobalt complexes **24**–**27**.

2.3. Homolytic versus Heterolytic: The Intrinsic Nature of the H_2 Evolution Step

Hydrogen evolution catalyzed by molecular complexes may occur through two distinct mechanisms.[45] In the homolytic mechanism (Figure 13, left), two metal hydride

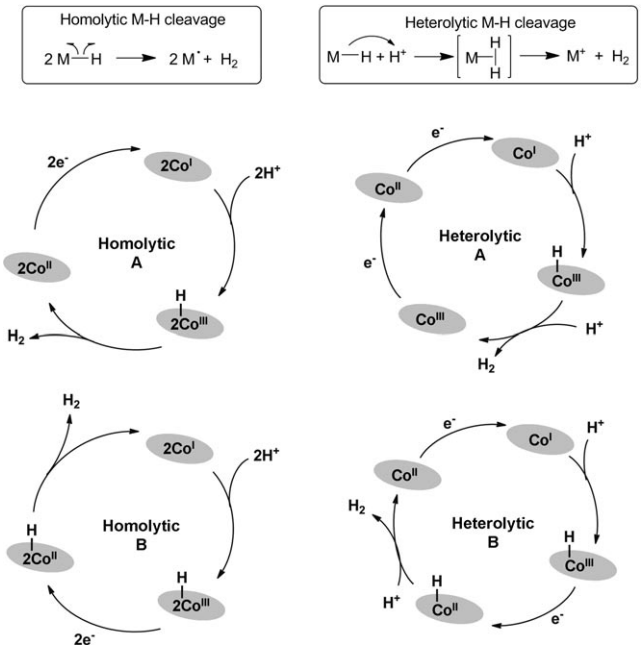

Figure 13. Homolytic and heterolytic mechanisms for H_2 evolution catalyzed by a molecular coordination compound.

complexes evolve H_2 by a reductive elimination reaction. In the course of the catalytic cycle, each metal center thus undergoes a monoelectronic reduction process, either before protonation (Figure 13, homolytic pathway A) or once the hydride species is formed (Figure 13, homolytic pathway B). In the alternative heterolytic pathway (Figure 13 right), the intermediate metal hydride decomposes by proton attack and evolves H_2 by an intermediate dihydrogen–metal σ complex. During the catalytic cycle, two electrons are transferred to the same metal center, either consecutively (Figure 13, heterolytic pathway A) or alternating with the two protonation steps (Figure 13, heterolytic pathway B).

A way to evaluate the potential of a given system to proceed homolytically or heterolytically is to study H_2 evolution from isolated hydride species, but as discussed above, this is only possible in a few cases. Furthermore, as shown below, both mechanisms very often operate simultaneously, with relative weights depending on reaction conditions. For example, the organometallic hydride $[CpCo^{III}(dppv)H]^{+}$ (Figure 10), stable in propylene carbonate solution, can be activated upon reduction by sodium amalgam or at an electrode held at −1.5 V versus SCE to quantitatively evolve hydrogen.[65] The mechanism is in this case obviously homolytic, as the reaction is carried out in the absence of protons. Addition of trifluoroacetic acid (TFA) to the solution after H_2 evolution has ceased allows the regeneration of the

hydride species with H_2 evolution under reductive electrochemical conditions. However, the detailed analysis of the kinetics of the reaction shows that both homolytic and heterolytic mechanisms now operate simultaneously. A similar reactivity is observed when $[CpCo^{III}(P(OMe)_3)_2H]^+$ catalyzes H_2 evolution from an aqueous solution at pH 5.[65]

Chao and Espenson carried out early studies on the reactivity of the isolated hydride compound $[HCo(dmgH)_2(PBu_3)]$ (Figure 11) with $HClO_4$ in methanol/water mixtures.[95] Under these conditions, $[HCo(dmgH)_2(PBu_3)]$ is protonated ($K = 1.3 \times 10^2\ mol^{-1}L$), probably at one oxime ligand, to yield $[HCo(dmgH_2)(dmgH)(PBu_3)]^+$. Both homolytic and heretolytic routes have been found to operate simultaneously. A high bimolecular rate constant of $1.7 \times 10^4\ mol^{-1}L\,s^{-1}$ has been determined for the first process. The rate constant for heterolytic hydrogen evolution is by comparison much more modest ($0.42\ mol^{-1}L\,s^{-1}$). Thus the heterolytic pathway is competitive only at low catalyst or high acid concentrations. Higher heterolytic rate constants are however expected for similar systems lacking the π-accepting axial phosphine ligand and thus having hydride intermediates that are more reactive towards protonation.

Kellet and Spiro developed a method to determine the equilibrium constants for both homolytic and heterolytic H_2 evolution from HA reduction for a catalyst under given conditions.[49] The method uses the redox potentials of the Co^{III}/Co^{II} and Co^{II}/Co^{I} couples and the standard potential of the $HA/^1/_2\,H_2 + A^-$ couple under the experimental conditons. While the first two values can be measured electrochemically, the last parameter can be calculated from tabulated data.[72,74,96]

Both pathways are considered as the sum of one H_2 evolution step [Eq. (4) or (5)][97] and one or two redox half-equations, as shown below:

Heterolytic route:

$$^1/_2\,[Co^I] + AH = {}^1/_2\,[Co^{III}] + {}^1/_2\,H_2 + A^-$$
$$^1/_2\,[Co^{III}] + e^- = {}^1/_2\,[Co^{II}]$$
$$^1/_2\,[Co^{II}] + e^- = {}^1/_2\,[Co^{I}]$$
$$\text{Net reaction}: \quad AH + e^- = {}^1/_2\,H_2 + A^- \qquad (4)$$

Thus,

$$\Delta_r G^\circ\ (1) - {}^1/_2\mathscr{F} \times E^\circ\ (Co^{III}/Co^{II}) - {}^1/_2\mathscr{F} \times E^\circ\ (Co^{II}/Co^{I})$$
$$= -\mathscr{F} \times E^\circ\ (H^+/H_2)$$

Homolytic route:

$$[Co^I] + AH = [Co^{II}] + {}^1/_2\,H_2 + A^-$$
$$[Co^{II}] + e^- = [Co^{I}]$$
$$\text{Net reaction}: \quad AH + e^- = {}^1/_2\,H_2 + A^- \qquad (5)$$

Thus,

$$\Delta_r G^\circ\ (2) - \mathscr{F} \times E^\circ\ (Co^{II}/Co^{I}) = -\mathscr{F} \times E^\circ\ (H^+/H_2)$$

This method was used to demonstrate that hydrogen evolution from $0.1\ mol\,L^{-1}$ aqueous TFA solution catalyzed by cobalt porphyrins proceeds from Co^{III}–H species through the homolytic route, with the protonation of the Co^I species being the rate determining step.[49] The same method has then been applied for various cobaloxime[48,51] and diimine-dioxime cobalt complexes.[55] In all of the calculations, the homolytic pathway is always found to be thermodynamically possible. The heterolytic process appears endergonic for BF_2-annulated complexes **9**, **10**, and **15**, but to various extents depending on the strength of the acid. In the case of the H-bridged complexes, either **12a** or **16**, this route was found to be thermodynamically favorable and likely to be competing with the homolytic route when strong acids are used. On the basis of simple kinetic–thermodynamic correlation considerations, Gray and co-workers proposed a lower value ($45\ kJ\,mol^{-1}$) for the barrier associated with heterolytic hydrogen activation. Note that such a value would just correspond to an activation energy of 250 mV for a two-electron process, which is of the same order of magnitude as that of the overpotential required by cobaloxime electrocatalysts. Thus, at the electrocatalytic potential, such a reaction can easily be driven by highly favourable electron-transfer processes between the electrode and the catalyst.

Additionally, digital simulations have been performed so as to identify which mechanism reproduces best the experimental cyclic voltammograms. The initial input of this approach was provided by Savéant and co-workers.[98] Simulations performed for different scan rates and in the presence of various amounts of Et_3NH^+ were consistent with heterolytic H_2 evolution catalyzed by **12a** and analogues with substituted pyridine ligands in DMF.[51] Similar simulations have been carried out for **9**, but they have led to some controversy between two groups.[48,52] Again, it should be noted that both mechanisms can occur simultaneously and/or predominate under distinct conditions (such as potential, concentration, and acid/catalyst ratio).

In the mechanisms discussed above, only the Co^{III}–H species has been considered as a possible intermediate. However, the latter can be reduced at the electrode so as to form a Co^{II}–H species that can itself evolve hydrogen through either the homolytic or the heterolytic route.[52,55] The lower oxidation state of the metal center destabilizes the hydride ligand and enhances its reactivity with acids. Such a species has thus been proposed to account for the slow hydrogen evolution catalyzed by **9** in the presence of weak acids, such as Et_3NH^+ in DMF or TFA in CH_3CN,[52] which are strong enough to protonate Co^I but not the Co^{III}–H intermediate.[99] This mechanism is also likely to operate in most of the light-driven H_2-evolving catalytic systems described in Section 3, as they require neutral to basic conditions.[100] Such a mechanism had been favored very recently by Gray and co-workers, which used proton transfer from the triplet excited state of brominated naphthol to the isolated Co^I species $\mathbf{9}^-$[101,102] and may also occur during hydrogen evolution from $[Co^I(do)(doH)pn(PPh_3)]$ (**36**; doH(doH)pn = N^2,$N^{2\prime}$-propanediyl-bis(2,3-butanone-2-imine-3-oxime)). The latter reacts with *p*-cyanoanilinium bromide as the proton source to yield half an equivalent of H_2 and the cobalt(II) complex $[Co(do)(doH)pnBr(PPh_3)]$ (Figure 14).[55] Acid-induced disproportionation of the Co^{II} species then generates Co^I and Co^{III} complexes (Figure 14), the former re-entering directly the catalytic cycle so that the net reaction is the stoichiometric formation of H_2 and a Co^{III} species from two protons and a

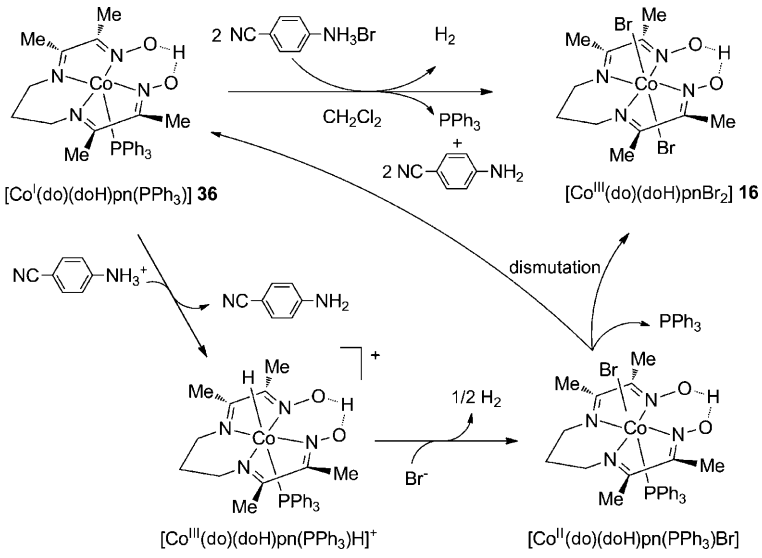

Figure 14. H_2 evolution from $[Co^{I}(do)(doH)pn(PPh_3)]$ (**36**).

Co^{I} complex.[55] Therefore, the observation of a Co^{III} intermediate cannot be used as an evidence for heterolytic H_2 evolution as recently claimed by Szajna-Fuller and Bakac.[90]

The design of catalytic systems functioning through a heterolytic pathway is a prerequisite for technological applications that will require immobilization of the catalyst onto an electrode substrate, as protonation of hydride sites at the surface should proceed smoothly (see Section 4). In contrast, mononuclear systems that evolve H_2 through a homolytic and thus bimetallic pathway should be inefficient when grafted on an electrode, as two different immobilized centers should not not be able to react together.[45,56] As a means to overcome these drawbacks, Peters recently developed bimetallic catalysts with the preparation of a series of pyridazine-templated dicobalt macrocycles **37** and **38** (Figure 15) in which each cobalt center is coordinated by two oxime and two imine ligands. These compounds can catalyze hydrogen evolution from 2,6-dichloroanilinium tetrafluoroborate in CH_3CN, although no indication about the catalytic mechanism is available.[69]

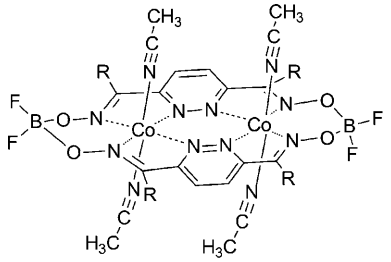

R = H **37**
R = Me **38**

Figure 15. Pyridazine-templated dicobalt macrocycles designed by Peters and co-workers.

2.4. Tuning the Electrocatalytic Performance

From a general point of view, catalysts requiring high overpotential (more than 400 mV) are of little interest for mid- or long-term technological water-splitting applications.[26,27,29] The same applies for systems with very negative electrocatalytic (that is, operating) potentials, even if they require a low overpotential, as the long-term aim is to work with aqueous electrolytes with a limited electrochemical window, even at carbonaceous electrodes.

2.4.1. Electrocatalytic Potential and Nucleophilicity

A large number of reports have considered the possibility of tuning the electrocatalytic potential through structural modification of the ligands in a series of catalysts. However, the modification of the coordination sphere not only influences the redox processes, but also the protonation/deprotonation steps. Unfortunately, both effects are opposite, as the presence of hard ligands for example facilitates the protonation of low-valent metal ions and enhances the hydridicity of metal hydride moieties, but decreases the potentials of the reduction steps.[45] As a general conclusion of these studies, it was stressed that "modification of the reduction potentials of a closely related set of catalysts, that is, varying remote substituents of the ligands, results in insignificant changes in the overpotential requirement for proton reduction":[103] species with a relatively positive reduction potential are also less nucleophilic and thus exhibit catalytic activity only under strongly acidic conditions. This point is well illustrated in the cobaloxime series: the redox potential is shifted by 380 mV to the more positive values when substituting glyoximato ($L = gH^-$) for dimethylglyoximato ($L = dmgH^-$) in $[Co^{II}(L)_2(py)]$, but $[Co(gH)_2(PBu_3]^-$ is approximately 600 times less nucleophilic than $[Co(dmgH)_2(PBu_3]^-$.[104] The same applies when considering substituting $dmgH^-$ in **9** by $dpgH^-$ in **10** or when switching from a proton-linked cobaloxime such as **11** to the BF_2-annulated compounds **9**.[51,52] Thus, whereas modifications in the equatorial bis(dioxime) ligand allow the electrocatalytic potentials to be tuned to keep the catalytic wave within a technologically relevant electrochemical window, this does not result in any improvement of the overpotential requirement, which remains in the 200–300 mV range under optimal conditions; that is, in the presence of sufficiently strong acid. A similar trend has been observed for complexes **4**–**6**. While the more electron-rich catalysts **3a,b** produce H_2 from *p*-toluenesulfonic acid with a turnover frequency of 10 h^{-1}, the diphenyl derivatives **4a,b** require a stronger acid, such as HBF_4, and only turn over 4 cycles per hour. The tetraphenyl derivatives **5a,b** are completely inactive for hydrogen evolution.[48]

2.4.2. Overpotential Requirement and Turnover Frequency

In the case of both tetraimine and porphyrin cobalt catalysts,[48,49] it has been observed that any electronic

modification at the catalytic center that lowers the overpotential requirement for H_2 evolution also leads to a decrease of the rate of catalysis. In the cobaloxime series, this statement is also valid for modifications at the equatorial plane. In contrast, modifications of the axial ligand *trans* to the hydride ligand involved in catalysis have a strong influence on the reactivity of the Co^{III}–H species and thus on the catalytic rate, whereas they have little influence if any on the electrochemical potential of the Co^{II}/Co^{I} couple, as with **11**–**14**, and on the electrocatalytic potential for hydrogen evolution.[51] This has been clearly demonstrated for the series **12**–**14a**: introduction of electron-withdrawing or electron-donating substituents in *para* position of the pyridine ligand strongly modifies the rate constant of the protonation of the Co^{III}–H bond (heterolytic hydrogen evolution) by several orders of magnitude. A linear correlation could be obtained between the rate constants of this step and the Hammett coefficients, which reflect the electronic properties of the substituents of the pyridine ligand.

2.4.3. Proton–Hydride Interaction

Structural modifications of the cobalt coordination sphere can also be inspired by natural systems, such as hydrogenase enzymes.[105] For example, introduction of basic sites close to the metal center may facilitate intra- and intermolecular proton transfer. If proton and electron transfer processes were efficiently coupled, a dramatic decrease of the overvoltage could be obtained. This approach has been initially and successfully developed by DuBois, Rakowsky DuBois, and co-workers with mononuclear nickel–bis(diphosphine) complexes, borrowing the nickel ion from the NiFe-hydrogenase metal center and taking the pendant proximal base, an amine group, but as part of a diphosphine ligand, from the active site of FeFe-hydrogenases.[106,107] Using the same diphosphine ligand with pendant amine functions for cobalt coordination yields $[Co(P^{Ph}{}_2N^{Ph}{}_2)(CH_3CN)_3]^{2+}$ (**34a**), a remarkable catalyst for hydrogen evolution from bromoanilinium tetrafluoroborate in acetonitrile with a turnover frequency of $90\,s^{-1}$ and an overpotential requirement of 285 mV.[67] Substituting *tert*-butyl for phenyl substituents on the cyclic phosphine ligand results in a positive shift of the $Co^{II/I}$ couple in **34b** and reduces the overpotential required for hydrogen evolution to 160 mV while increasing the turnover frequency to $160\,s^{-1}$.[68] A cobalt complex with a related diphosphine ligand that does not contain a pendant base is not catalytically active. The analogue **34c**, with a more basic amine is also not active.[108]

The importance of a basic site in the second coordination sphere has also been shown in the case of diimine-dioxime cobalt complexes **16** and **17**, which contain a proton bridging two N-bound oxime functions and are susceptible to proton exchange.[55] These complexes are indeed excellent electrocatalyts for proton reduction into H_2 at small overpotentials. Protonation at this OH···O bridge, yielding a species bearing two protonated oxime ligands, has been proposed to account for the anodic shift of the electrocatalytic wave for hydrogen evolution with regard to the Co^{II}/Co^{I} potential in the presence of strong acid. Indeed, this is not observed for the BF_2-annulated analogue **15**.[55] Here, the presence of an H^+-exchanging site provides the catalyst with a mechanism to adjust its electrocatalytic potential for hydrogen evolution to the acid–base conditions of the solution and allows the overvoltage for the reduction of acids to be kept within reasonable values over a wide range of pK_a values. Such a progressive shift of the electrocatalytic potential as a function of the strength of the proton source used has never been observed for a synthetic molecular catalyst. Similarly, hydrogenase enzymes[12] have this ability to adapt their electrocatalytic potential by modifying their surface charge through protonation and thus to catalyze H_2/H^+ interconversion near the equilibrium over a wide range of pH values.[109] Whether such an open oxime bridge is involved in the proton transfer steps along the catalytic cycle for hydrogen evolution, thus promoting fast Co^{III}–H formation and/or accelerating its protonation by a proton–hydride interaction, has not been studied to date. It should be noted that such a protonated cobaloxime intermediate with an open oxime bridge has been previously seen during the course of heterolytic hydrogen evolution (Figure 11).[95]

These examples demonstrate that an increased understanding of the chemical principles on which the reactivity of a biological active site is built on, together with a fine utilization of the synthetic power of chemistry, allow for minor modifications of a bioinspired catalyst, thus resulting in considerable functional improvements.

2.5. Conclusions

Cobalt-based hydrogen evolution catalysts have received growing interest in the past five years. In particular, cobaloximes and diimine-dioxime cobalt complexes are some of the most efficient catalytic systems as far as overpotential requirement, turnover frequency, and robustness are concerned. They have also found application in the design of light-driven hydrogen evolution systems, which will be described in Section 3.

3. Cobalt-Based Photocatalytic H_2-Evolving Systems

The second issue for the design of an artificial system for water splitting resides in using sunlight directly as the energy source for driving H_2 generation, thereby mimicking the direct light-to-chemical energy transduction achieved by photosynthetic organisms. This process requires the efficient coupling of an H_2-evolving catalyst with a photosensitizer.[110] The latter converts the luminous flux into a flow of electrons (wireless current) to be used by the catalytic center. The cobalt-based systems described in Section 2 have been among the most employed systems for the construction of light-driven systems for H_2 evolution. In this section, we will first describe multicomponent systems consisting of isolated photosensitizers and H_2-evolving catalysts and then supramolecular assemblies combining the two functions. We will not discuss systems for which H_2 evolution has only been noticed as a side reaction of (or together with) CO_2 photo-

reduction.[111–115] Furthermore, and because we consider that multielectron catalysis is a key issue in these systems, we exclusively present turnover numbers relative to the amount of cobalt catalyst present in solution, even if the latter is in excess with regard to the photosensitizer.

The general mechanisms for light-driven H_2-evolution catalyzed by cobalt systems are shown in Figure 16. The process is initiated in any case by the absorption of a photon

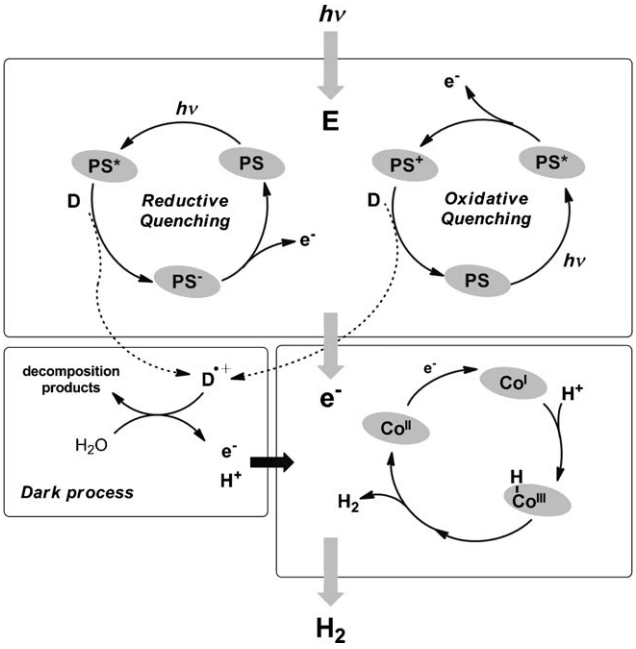

Figure 16. PS-based, cobalt-based, and dark processes involved in light-driven H_2 evolution catalyzed by cobalt complexes.

by the photosensitizer, yielding a PS* excited state. From this state, a first photoinduced electron transfer may take place by an oxidative quenching process involving the cobalt complex as the electron acceptor and generating the active Co^I species. A second electron transfer process then occurs between the sacrificial electron donor and the resulting oxidized photosensitizer PS^+, thus regenerating the PS. An alternative mechanism implies a reductive quenching of the PS* by the sacrificial electron donor first to yield the reduced PS^-, which subsequently reduces the catalyst to the Co^I state. In the specific case of the Co^{III} catalysts, a primary photoinduced electron transfer step is necessary to generate the Co^{II} complex that is further reduced to the Co^I state. This was suggested to be responsible for the existence of an induction period.[116,117]

The establishment of one mechanism versus the other will essentially depend on the redox properties of the different couples (PS^+/PS^*, PS^*/PS^-, Co^{III}/Co^{II}, Co^{II}/Co^I, $D^{\bullet+}/D$), and their relative concentrations (see Section 3.3).

Some electrons entering the cobalt catalytic cycle might originate from a dark (thermal) process that is different from the light-induced process; indeed, in most of these photocatalytic experiments, the sacrificial electron donor is an amine (triethanolamine, TEOA, or triethylamine, TEA). After electron transfer (either to PS* or to PS^+), a radical cation is formed, which is known to decompose in the reaction medium to give one equivalent of proton and one equivalent of electron, together with aldehyde and secondary amine byproducts (Figure 16).[118–120] This dark process should be considered practically in determining the quantum yield for the photoproduction of H_2.

3.1. Multicomponent Photocatalytic Systems

Until the late 1970s, most of the work in this area relied on the use of $[Ru(bpy)_3]^{2+}$ (**PS1**; Figure 17) as the photosensitizer in combination with platinum colloids as the heterogeneous

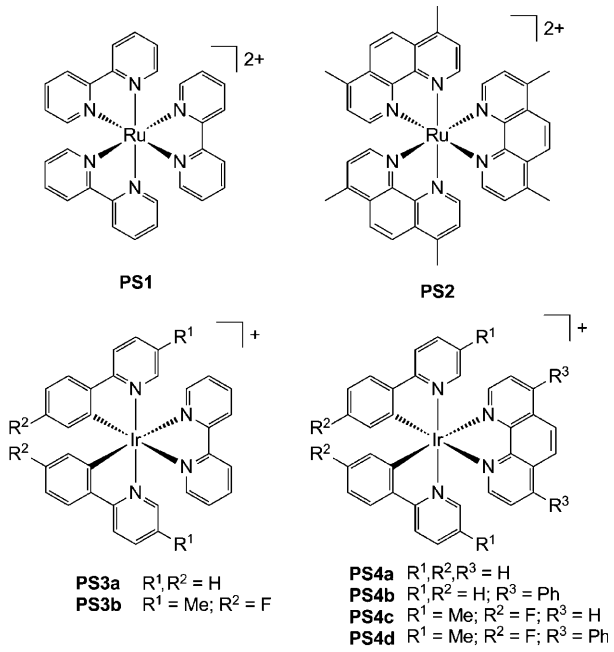

Figure 17. Structures of photosensitizers employed in combination with the $[Co(bipy)_n]^{2+}$ H_2-evolving system.

H_2-evolving catalyst.[121,122] In these systems, cobalt complexes were initially employed as electron relays[123] alternative to methyl viologen.[118,124,125] However, control experiments revealed that in that case, hydrogen could also be evolved in the absence of a Pt catalyst.[115,118] Importantly, these early reports have revealed that in the case of homogeneous cobalt-based hydrogen photoproduction, and in contrast with systems based on platinum colloids, no electron mediator needs to be employed.

Following these pioneering observations, a wide range of cobalt complexes, ranging from $[Co(bipy)_n]^{2+}$ species ($n = 1$–3; Figure 5)[57,115,126–128] to the cobalt–polypyridinium complexes **39** and **40** (Figure 18)[129] to some macrocyclic Co^{II} complexes, including **1**,[130] that are based on the ligands shown in Figure 19[130,131] or the cobaloxime **11**[131] have been used.[132]

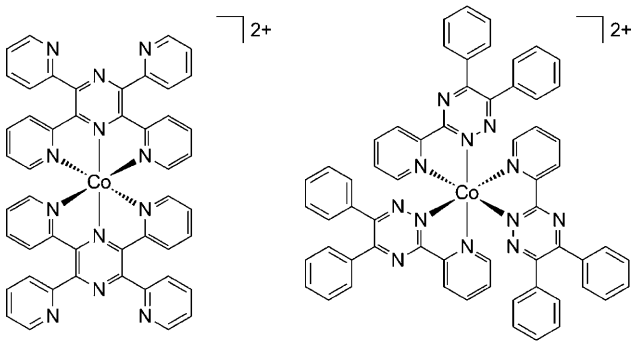

39 40

Figure 18. Structures of the cobalt polypyridinium complexes **39** and **40**.

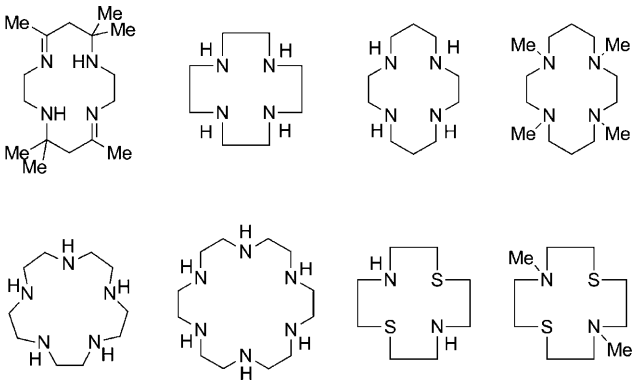

Figure 19. Representative structures of macrocyclic ligands employed in cobalt-based H_2-evolving complexes in combination with **PS1**.

3.1.1. Systems with $[Co(bipy)_3]^{2+}$

The combination of Co^{II} ions and bipy ligands for H_2 photoproduction has been extensively studied by Sutin and co-workers.[57–60,127] Visible-light-induced hydrogen production has been demonstrated from aqueous solution when these two components were mixed with **PS1** and ascorbate in large excess as the sacrificial electron donor at the optimum pH of 5.[127] Formation of dihydropyridine as a consequence of the reduction of bipy ligand has been noticed as a side reaction. When bipy is replaced by 4,4′-dimethylbipyridine in the catalytic system, a considerably higher quantum yield for H_2 production is obtained.[127] This work has been further improved by using $[Ru(dmphen)_3]^{2+}$ (**PS2**) as the photosensitizer, TEOA as the sacrificial electron donor, and $[Co(bipy)_3]^{2+}$ (Figure 5) as the catalyst precursor in a 1:1 mixture of CH_3CN and H_2O at pH 8.[57]

Recently $[Co(bpy)_3]^{2+}$ was associated with various cyclometallated diimine–iridium complexes (**PS3** and **PS4**; Figure 17), prepared by a combinatorial method, in water/acetonitrile mixtures in the presence of LiCl and with TEOA as the sacrificial electron donor.[133] Under the conditions used, eight turnovers based on $[Co(bpy)_3]^{2+}$ are achieved by the photocatalytic system, with no significant variation depending on the iridium-based photosensitizer structure, while **PS1** only allows one turnover. However, use of the ruthenium-based **PS2** instead of **PS1** allows the efficiency to be improved by a factor of 6; as stated above, this trend in the Ru series has been observed by Sutin and co-workers.[57]

3.1.2. Multicomponent Systems with Cobaloxime Catalysts

Since 2008, the design of new photocatalytic systems has focused on the use of cobaloximes as H_2-evolving catalysts (Table 2).[134] However, the first application of a cobaloxime catalyst (**11**; Figure 3) in combination with **PS1** was reported in 1983 by Lehn and co-workers, with about 16 TON h^{-1} achieved in a DMF/H_2O solution with apparent pH ≈ 9.[131] TEOA was used as the sacrificial electron donor. Excess of free $dmgH_2$ ligand was found to be necessary to replace hydrogenated ligand formed by side reactions and sustain the activity. Addition of one equivalent of P*n*Bu_3 provides enhanced stability to the photocatalytic system, resulting in a TON of up to 88. The use of the more stable BF_2-annulated cobaloxime **9** with **PS1** was reported in 2008, with a TON of 20 achieved within one hour in acetone with TEA as the sacrificial electron donor and triethylammonium ($HTEA^+$) tetrafluoroborate salt as the proton source.[100] Under these conditions, a very low activity was found for the initial catalytic system reported by Lehn (Table 2). This result shows that such homogeneous photocatalytic systems are extremely sensitive to the experimental conditions and in particular to the composition of the media, the proton source or apparent pH, and the nature of the sacrificial electron donors. We will discuss these issues in detail below.

Systems based on cobaloxime **9** as the H_2-evolving catalyst were further improved by the use of other metal-based photosensitizers, such as the cyclometallated iridium diimine **PS4a** (Figure 17) or the tricarbonylrhenium diimine **PS5a** (Figure 20),[135] resulting in H_2 production with 165 (15 h) and 273 (15 h) TON, respectively. The organic dye **PS9** has also been used.[136] Cobalt diimine-dioxime catalysts[55] have also been integrated into photochemical H_2-evolving systems based on cyclometallated iridium diimine **PS3a**.[137] Table 2 collects the photocatalytic performances, together with the experimental conditions, of the various systems based on a cobaloxime reported to date.

Eisenberg and co-workers used the H-bridged cobaloxime bearing an axial pyridine ligand **12a** together with a series of platinum chromophores **PS6a–d**.[116,117,139] Under their standard experimental conditions (CH_3CN/H_2O, 3:2; TEOA 0.16 mM), the rate of hydrogen generation follows the order **PS6d** > **PS6b** > **PS6c** > **PS6a**. Cyclometallated derivatives **PS7a–c** proved less efficient, with the most efficient derivative, **PS7a**, being comparable to **PS6a**.[116,117] Improved performances could be obtained either by modifying the solvent mixture (Table 2, entry 8) or by employing a higher concentration of TEOA (Table 2, entry 9), allowing up to 120 TON_{Co} (2150 turnovers with respect to the Pt sensitizer; Table 2, entry 10) during a 10 h experiment. In a similar study, Castellano and co-workers established the influence of the phenylacetylide π-conjugation length in **PS6e,f** on the photocatalytic activity of systems based on **12a**.[140] In these studies, no free $dmgH_2$ ligand is introduced in excess to repair the catalyst, which may decompose during catalysis.

Table 2: Photocatalytic performances of multicomponent systems with cobalt-based H_2-evolving catalysts.

Entry	PS		Cat.	PS/Cat.	Solvent	pH_{app}	Light	t[e]	TON_{Co}[f]	Φ[g]	Ref.
1	Ru	**PS1**	**11**[a]	1:2.4	DMF/TEOA, 2:1	8.8	$\lambda > 400$ nm	1 h	16	$\geq 13\%$	[131]
2		**PS1**	**11**[a]	1:2.4	DMF/TEOA, 2:1 + 1 equiv P*n*Bu$_3$	10.4	$\lambda > 400$ nm	6.5 h	88		[131]
3		**PS1**	**11**[a]	1:2	DMF TEOA, AcOH	–	$\lambda > 400$ nm	9 h	33		[138]
4		**PS1**	**9**	1:1	acetone, TEA [HTEA][BF_4][b]	–	white light $\lambda > 350$ nm	1 h	20		[100]
5		**PS1**	**11**[a]	1:2.4	acetone, TEA [HTEA][BF_4][b]	–	white light $\lambda > 350$ nm	4 h	2		[100]
6	Ir	**PS4a**	**9**	1:1	acetone, TEA [HTEA][BF_4][c]	–	$\lambda > 380$ nm	15 h	165	10%	[135]
7		**PS3a**	**16**	1:1	MeCN/H_2O, 1:1 TEA (10%)	10	$\lambda > 400$ nm	4 h	307		[137]
8		**PS3a**	**16** + PPh_3	1:1	MeCN/H_2O, 1:1 TEA (10%)	10	$\lambda > 400$ nm	10 h	696		[137]
7	Pt	**PS6a**	**12a**	1:18	MeCN/H_2O, 3:2 TEOA (0.16 M)	8.5	$\lambda > 410$ nm	5 h	11		[116, 117]
8		**PS6a**	**12a**	1:18	MeCN/H_2O, 24:1 TEOA (0.16 M)	8.5	$\lambda > 410$ nm	5 h	22		[116, 117]
9		**PS6a**	**12a**	1:18	MeCN/H_2O, 3:2 TEOA (0.27 M)	8.5	$\lambda > 410$ nm	10 h	56		[139]
10		**PS6a**	**12a**	1:18	MeCN/H_2O, 24:1 TEOA (0.27 M)	8.5	$\lambda > 410$ nm	10 h	120		[116, 117]
11		**PS7a**	**12a**	1:18	MeCN/H_2O, 3:2 TEOA (0.16 M)	8.5	$\lambda > 410$ nm	5 h	9		[116, 117]
12		**PS6a**	**12b**	1:18	MeCN/H_2O, 3:2 TEOA(0.16 M)	8.5	$\lambda > 410$ nm	5 h	7		[116, 117]
13		**PS6a**	**13**	1:18	MeCN/H_2O, 3:2 TEOA (0.16 M)	8.5	$\lambda > 410$ nm	5 h	6		[116, 117]
14		**PS6a**	**14b**	1:18	MeCN/H_2O, 3:2 TEOA (0.16 M)	8.5	$\lambda > 410$ nm	5 h	13		[116, 117]
15		**PS6a**	**35**	1:18	MeCN/H_2O, 3:2 TEOA (0.16 M)	8.5	$\lambda > 410$ nm	5 h	<1		[116, 117]
16		**PS6a**	**9**	1:18	MeCN/H_2O, 3:2 TEOA (0.16 M)	8.5	$\lambda > 410$ nm	5 h	<1		[116, 117]
17		**PS6e**	**12a**	1:18	MeCN/H_2O, 1:1 TEOA (0.5 M)	8.5	$\lambda > 420$ nm	3 h	44	17%	[140]
18		**PS6e**	**12a**	1:18	MeCN/H_2O, 1:1 TEOA (0.5 M)	8.5	442 nm	1 h	4	17%	[140]
19		**PS6f**	**12a**	1:18	MeCN/H_2O, 1:1 TEOA (0.5 M)	8.5	442 nm	1 h	5	16%	[140]
20		**PS6g**	**12a**	1:18	MeCN/H_2O, 1:1 TEOA (0.5 M)	8.5	442 nm	1 h	7	15%	[140]
21	Re	**PS5a**	**9**	1:1	acetone, TEA [HTEA](BF_4)[c]	–	$\lambda > 380$ nm	15 h	273	16%	[135]
22		**PS5b**	**11**[a]	1:2	DMF TEOA, AcOH	–	$\lambda > 400$ nm	9 h	75	26%	[138]
23		**PS5c**	**11**[a]	1:17	DMF, TEOA [HTEOA](BF_4)[d]	–	LED 380 nm	120 h	353		[120]
24		**PS5c**	**11**[a]	1:1	DMF, TEOA [HTEOA](BF_4)[d]	–	LED 476 nm	120 h	1850	ca. 90%	[120]
25	no	**PS8**	**12a**[a]	1:5	MeCN/H_2O, 1:1 TEOA (5%)	7	$\lambda > 450$ nm	12 h	180	4%	[141]
26	metal	**PS9**	**12a**[a]	1:5	MeCN/H_2O, 1:1 TEOA (5%)	7	$\lambda > 450$ nm	12 h	90		[141]
27		**PS9**	**9**	4:1	MeCN/H_2O, 1:2 TEA (10%)	10	$\lambda > 400$ nm	5 h	327		[136]
28		**PS9**	**10**	4:1	MeCN/H_2O, 1:2 TEA (10%)	10	$\lambda > 400$ nm	5 h	25		[136]

Table 2: (Continued)

Entry	PS	Cat.	PS/Cat.	Solvent	pH_{app}	Light	t[e]	TON_{Co}[f]	Φ[g]	Ref.
29	**PS10b**	**12a**	1:124	MeCN/H_2O, 1:1 TEOA (5%)	7	$\lambda > 455$ nm	24 h	ca. 36	12%	[142]
30	**PS10c**	**12a**[a]	1:74	MeCN/H_2O, 1:1 TEOA (5%)	7	$\lambda > 455$ nm	24 h	127	33%	[142]

[a] An excess of $dmgH_2$ ligand is added. [b] 300 equiv TEA + 300 equiv [HTEA](BF_4). [c] 600 equiv TEA + 600 equiv [HTEA](BF_4). [d] [HTEOA](BF_4) is prepared in situ by mixing [HBF_4] (0.1 M) and [TEOA] (1 M). [e] Turnover number relative to cobalt. [g] Quantum yield.

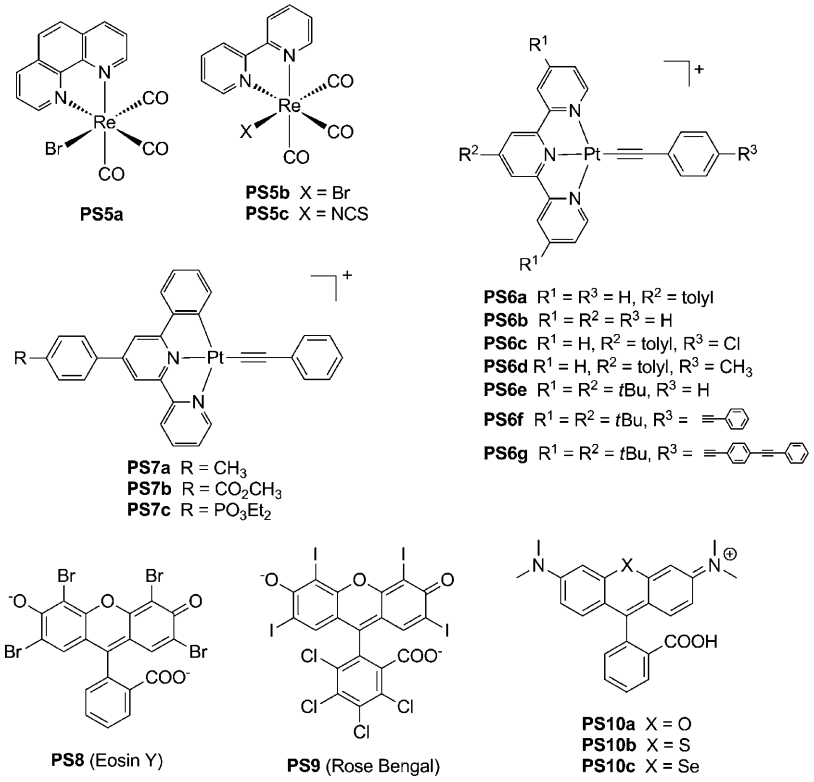

Figure 20. Structures of various photosensitizers used in combination with cobaloxime H_2-evolving catalysts.

The photocatalytic performances of various cobaloxime catalysts (**9**, **12**–**14**, **35**), in association with **PS6a**, have also been determined; the best activities were obtained with **14b**, which contains a pyridyl ligand substituted by an electron-withdrawing group (Table 2, entry 16).[116,117] This observation contrasts significantly with the results obtained by Artero and co-workers in their former electrocatalytic study, where the highest activities were obtained with electron-donor-substituted cobaloximes, such as **13**.[51] This suggests that cobalt-centered catalysis may not be the rate-determining step in light-driven H_2 evolution.

Alberto and co-workers recently re-examined the use of cobaloxime **11** specifically in combination with tricarbonylrhenium–diimine sensitizers.[120,138] Using **PS5b**, TEOA as the sacrificial electron donor and acetic acid as the proton source in DMF, a TON of 75 was achieved after 9 h irradiation ($\lambda >$ 400 nm).[138] Importantly, a high quantum yield (40%) was measured in the initial stage of the reaction. Exchanging the bromide ligand in **PS5b** by a thiocyanate ligand yields an improved system that is able to achieve a TON of up to 353 in a 120 h experiment.[120] Upon replacement of acetic acid by HBF_4, yielding [HTEOA]BF_4, the apparent quantum yield for hydrogen production reaches 90% at 380 nm. However, the actual quantum yield might be smaller (ca. 45%) if reducing equivalents produced during the dark process (Figure 16) are taken into account.[120] Turnovers up to 1850 per cobalt ion (ca. 300 per $dmgH_2$ ligand added to the solution to restore the integrity of the catalyst) could be achieved under these conditions, which is the highest efficiency reported to date for a cobaloxime-based photocatalytic system.

As a major breakthrough, in 2009 Eisenberg and co-workers reported the first homogeneous system exclusively based on earth-abundant elements.[141] In this system, the noble-metal-based photosensitizers were replaced by organic dyes, such as Eosin Y (**PS8**) or Rose Bengal (**PS9**). Other xanthene derivatives, such as fluoresceine, lacking heavy bromide or iodide substituents, were not active under photocatalytic conditions. Actually, the presence of heavy atoms facilitates intersystem crossing and thus production of a long-lived triplet state required for the efficient transfer of electrons to the catalyst. The highest TON (180) was obtained with **PS8** and catalyst **12a** in the presence of a 12-fold excess of free $dmgH_2$ ligand. H_2 production ceased after 12 h of irradiation, coinciding with bleaching of the photolysis solution. **PS9** was found efficient under the same conditions but less photostable. This photosensitizer was also examined by Wang, Sun, and co-workers in combination with BF_2-annulated cobaloximes **9** and **10**.[136] Catalyst **9** was the most efficient, with 327 turnovers achieved within 5 h. Injection of **PS9** into the photolysis solution restored the activity and allowed about 150 additional turnovers. Catalyst **10**, with phenyl substituents at the dioxime ligands, is less active despite a larger driving force in the electron transfer from the excited PS, probably because of its lower nucleophilicity.[52,100] In these experiments,[136,141] the presence of Co^I is seen by a strong visible absorption near 600 nm. The clathrochelate complexes **28** and **29** were also assayed under similar conditions and were about four times less active than **9**. Eisenberg and co-workers further improved their photocatalytic system by replacing the fluorescein-based dye Eosin Y **PS8** by rhodamine dye ana-

logues containing S or Se in place of O in the xanthene ring (**PS10a–c**).[142] These synthetic modifications confer higher stabilities to the dye, and up to 9000 turnovers with respect to the sensitizer are reached under optimized conditions; however, this corresponds to a TON of only 127 versus Co, and an excess of $dmgH_2$ ligand is necessary to keep the system active over a 24 h period under irradiation (bleaching is observed after 3 h without added $dmgH_2$).

3.2. Supramolecular Cobaloxime-Based Photocatalysts

This field was initiated in 2008 from our reports on a series of supramolecular photocatalysts (**41–43**; Figure 21) for H_2 production based on cobaloxime centers.[100,135] These heterodinuclear ruthenium cobaloxime photocatalysts were obtained by axial cobalt coordination of a pyridine-functionalized ruthenium–diimine photosensitizer. Their activity can be tuned through manipulation of 1) the Co coordination sphere (compare **41a** with **41b**, or with **42**, in Table 3) and 2) the linker (compare **41a** with **41c**, **44** with **45**, and **47a–d** in Table 3). These studies show that supramolecular assemblies are more active than the corresponding multicomponent systems[100] and that a conjugated bridge is not essential.[143] Compound **41a** achieved 103 turnovers in the course of a 15 h experiment, which is competitive with previously reported Ru–Pt,[144,145] Ru–Pd,[146,147] and Ru–Rh[148] supramolecular systems containing noble-metal-based catalytic centers or the dirhodium photocatalyst $[Rh_2(dfpma)_3(PPh_3)(CO)]$ (dpfma = bis(difluorophosphino)methylamine) developed by Nocera and co-workers.[149] As a major drawback and for still unknown reasons, compounds **41a–c** and **42** require near-UV light to drive H_2 evolution. In contrast, **43**, which bears substituted phenanthroline ancillary ligands on the Ru center, is active under pure visible-light irradiation.[135]

Another component that can be modulated is the photosensitizing unit. Compound **46** with an iridium-based dye achieves a TON of 210 in the course of a 15 h experiment (Table 3, entry 8),[135] in good agreement with the observed superiority of iridium over ruthenium photosensitizers.[133] Again the supramolecular architecture is more stable than the two-component catalytic system composed of **9** and **PS9**, which levels off after 165 turnovers (Table 2, entry 6). As the two-component and supramolecular systems display comparable initial turnover frequencies, electron transfer from the photosensitizer to the cobalt center is not likely to be the rate-determining step.

Another strategy recently developed by Sakai and co-workers relies on the spontaneous self-assembly of bipy-appended cyclometallated Ir photosensitizers in the presence of Co^{II} ions, thus generating $[Co(bipy\text{-}L\text{-}Ir)_n]^{2+}$-type species in situ (**47**; Figure 21).[150] In the presence of TEOA, these systems mediate light-driven H_2 production in CH_3CN/H_2O mixtures with a TON of up to 20 (Table 3, entries 9–12). H_2 generation is significantly affected by the CH_3CN/H_2O ratio, the TEOA concentration, and the nature of the spacer between the PS and the Co core. Multicomponent systems tested under the same experimental conditions proved to be half as efficient, again pointing out the importance of the supramolecular system.

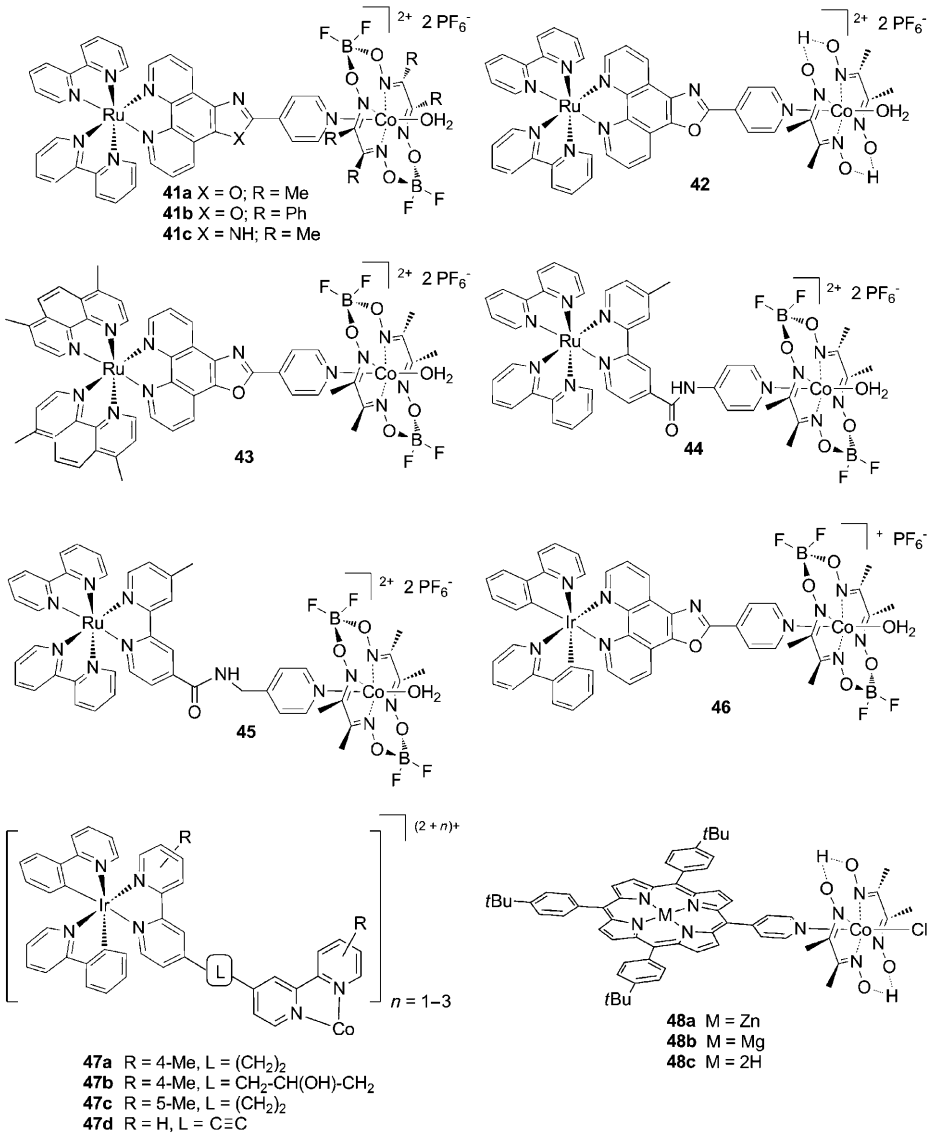

Figure 21. Structures of supramolecular cobaloxime-based H_2-evolving photocatalysts.

Table 3: Photocatalytic performances of cobalt-based supramolecular H_2-evolving catalysts.

Entry	Cat.	Conditions	t[a]	Light	TON	Ref.
1	**41a**	acetone, TEA [HTEA](BF$_4$)	4 h 15 h	white light $\lambda > 350$ nm	56 103	[100]
2	**42**	acetone, TEA [HTEA](BF$_4$)	4 h	white light	17	[100]
3	**41b**	acetone, TEA [HTEA](BF$_4$)	4 h	white light	12	[100]
4	**41c**	acetone, TEA [HTEA](BF$_4$)	4 h	white light	104	[100]
5	**43**	acetone, TEA [HTEA](BF$_4$)	4 h	$\lambda > 380$ nm	9	[135]
6	**44**	acetone, TEA [HTEA](BF$_4$)	8 h	$\lambda > 400$ nm	38	[143]
7	**45**	acetone, TEA [HTEA](BF$_4$)	8 h	$\lambda > 400$ nm	48	[143]
8	**46**	acetone, TEA [HTEA](BF$_4$)	15 h	$\lambda > 380$ nm	210	[135]
9	**47a**[b]	MeCN/H$_2$O, 1:1 TEOA (15 mM)	8 h	$\lambda = 400$–700 nm	20	[150]
10	**47b**[b]	MeCN/H$_2$O, 1:1 TEOA (15 mM)	8 h	$\lambda = 400$–700 nm	8	[150]
11	**47c**[b]	MeCN/H$_2$O, 1:1 TEOA (1.2 M)	8 h	$\lambda = 400$–700 nm	3.9	[150]
12	**47d**[b]	MeCN/H$_2$O, 1:1 TEOA (1.2 M)	8 h	$\lambda = 400$–700 nm	2.5	[150]
13	**48a**	THF/H$_2$O, 8:2 TEA	5 h	$\lambda > 400$ nm	22	[151]
14	**48b**	THF/H$_2$O, 8:2 TEA	5 h	$\lambda > 400$ nm	3	[151]
15	**48c**	THF/H$_2$O, 8:2 TEA	5 h	$\lambda > 400$ nm	< 1	[151]

[a] Illumination time. [b] The supramolecular assembly is prepared by mixing in situ $CoCl_2$ with 3 equiv of the bipy-appended iridium complex.

Finally, noble-metal-free supramolecular devices have been reported by the group of Wang and Sun.[151] They assembled pyridyl-functionalized porphyrin photosensitive units to a cobaloxime complex by axial cobalt coordination (Figure 21; **48a–c**). Modification in the central atom of the porphyrin results in drastic variations of the photocatalytic activity: whereas small amounts of H_2 are detected with either the Mg porphyrin **48b** or the free-base porphyrin **48c**, TONs of up to 22 are achieved with the Zn-based device **48a** in a 5 h experiment. On the basis of spectroscopic studies, the authors suggest that an axial weak coordination of TEA to Zn could account for the highest performance of **48a** through an inner-sphere electron transfer process. Under the same experimental conditions, a three-component catalytic system ([Zn(PyTBPP)] + **12a** + TEA) does not evolve any detectable amount of H_2.

In a recent study, Tiede et al. compared, in terms of ground state CH_3CN-phase structures and excited-state characteristics, three new axially coordinated cobaloxime-based supramolecular structures (Figure 22) containing distinct photosensitive moieties, such as ruthenium(II) bis(terpyridyl) in **49** and **50** and perylene-3,4:9,10-bis(dicarboximide) (PDI) in **51**.[152] An equilibrium is observed between the axially coordinated supramolecular assembly and the dissociated cobaloxime and PS fragments, with **49** retaining 90% of its integrity and **51** only 19%. Furthermore, a phenothiazine (PTZ) donor moiety on the PS fragment in **50** was introduced to stabilize the charge-separated state within oxidized PTZ and reduced cobaloxime by a push–pull effect. These systems have not yet been tested for photocatalytic hydrogen production.

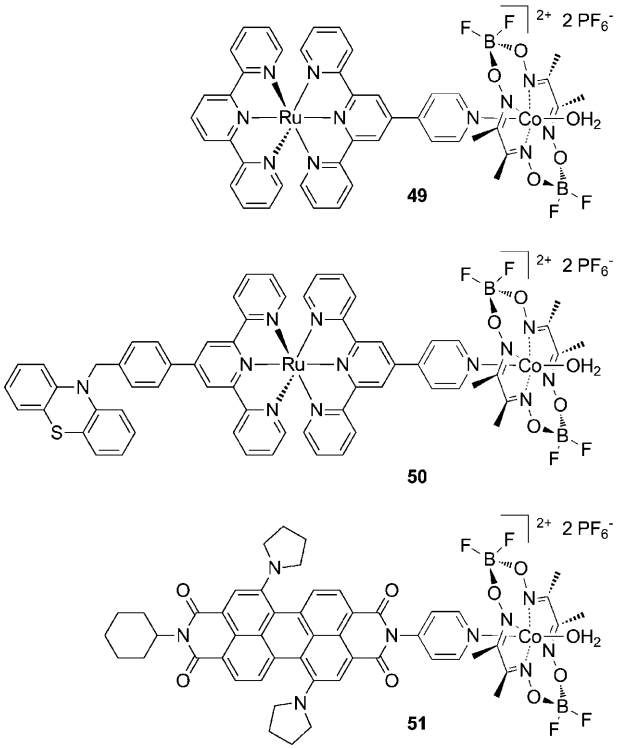

Figure 22. Cobaloxime-based supramolecular assemblies studied by Tiede et al.[152]

The weakness of the coordination bond between the PS and the cobaloxime fragments is thus a major drawback of these systems. Next generations of supramolecular assemblies, in particular targeting the development of efficient and stable photocathodes in photocatalytic devices, will necessitate a covalent attachment of the two fragments.

A system recently appeared in which the cobaloxime **14c** and the photosensitizer [Ru(bipy)$_2${2,2′ bipyridine-4,4′-diylbis(phosphonic acid)}]$^{2+}$ are electronically connected by a TiO_2 particle.[153] Both molecules with phosphonate anchoring groups are grafted onto the suface of TiO_2 with a ratio PS/catalyst = 3. Hydrogen (TON 53) is evolved when this system is placed in pH 7 TEOA aqueous buffer and exposed to visible light. This design takes advantage of the ultrafast electron injection from the excited state of the photosensitizer into the conduction band of TiO_2, from which they may be further transferred to the catalyst. Direct electron transfer was however not discarded. It however still suffers from photoinstability of the ruthenium dye.

3.3. Influence of the Various Experimental Parameters

Optimization of PS/catalyst combinations is not a trivial process. Indeed, photocatalytic efficiency strongly relies on a

broad range of parameters (such as solvent, apparent pH, nature of the sacrificial electron donor) that cannot be optimized independently. Thus when experimental conditions have been optimized for a given system, it is difficult to transpose them to another system.

Pronounced solvent effects are observed for all of the photocatalytic systems that have been described in the literature. DMF, CH_3CN, or acetone appear to be solvents of choice, generally in combination with water (up to 66%). For these mixed solvents, it is often claimed that water acts as the proton source, although protonated forms of TEA or TEOA should also be considered. Even though such solvent mixtures with water provide a first step towards using water as a solvent in applications for water photolysis, the systems reported above are generally inactive when assayed in pure aqueous buffers. To date, and to the best of our knowledge, combinations of **PS9** with **9** (10% aqueous TEA, pH 10; 21 turnovers achieved within 5 h)[136] and of **PS1** with $[Co(bipy)_3]^{2+}$[127] are the only cobalt-based photocatalytic systems reported to evolve H_2 in aqueous solution.

The acidity of the medium is perhaps the most important parameter to consider in the optimization of the photocatalytic reaction conditions. Sometimes, the authors measure an apparent pH with a glass electrode.[131] It should be noted that apparent pH is not well defined in a non-aqueous mixture and its determination is difficult to carry out reproducibly as the linearity of the response of a glass electrode is only warranted in water solutions of $pH \leq 12$. Other groups measure the pH of a 10% v/v aqueous solution of TEA or TEAO before mixing it with CH_3CN.[117,141] In that case, the apparent pH may vary significantly with the composition of the final medium. In any case, a strong dependence of pH is observed for most light-driven H_2-evolving systems.[120,131,136,138,139,141] No H_2 production was generally observed if the pH_{app} value was lower than 6–8 or higher than 12–13. At low pH values, protonation of TEA or TEAO decreases the amount of the redox-active basic form acting as sacrificial electron donor for regeneration of the photosensitizer. At more basic pH values, protonation of the Co^I catalyst becomes unfavourable.[131,154] Eisenberg and co-workers have shown that for systems based on the same cobalt catalyst (**12**) and sacrificial electron donor (TEOA) in CH_3CN/H_2O mixtures, maximal TONs are obtained at pH_{app} 8.5 using **PS6** platinum photosensitizers,[117,139] whereas the optimal pH_{app} is about 7 with **PS8**.[141] As the notion of pH is difficult to define in non-aqueous solvent, Alberto and co-workers use the ratio between the acid (CH_3COOH or HBF_4) and the basic sacrificial electron donor concentrations as a parameter. Alternatively, a form of buffer can be made by introducing equimolar amounts of the sacrificial electron donor and of its conjugated acid, such as TEA/[HTEA][BF_4], as done in our studies.[100,135]

Finally, deactivation of the system is often observed after several hours, but generally not understood at the molecular level. Production of Co nanoparticles, deprived of any H_2-evolving activity,[117] is a possibility that cannot be excluded as it has been observed for noble-metal-based catalytic systems.[155] Bleaching of the catalyst is the major cause of inactivation in the case of systems based on organic dyes.[136,141] Metal–diimine photosensitizers, such as **PS1**, are also known to photodecompose,[131] but rhenium-based photosensitizers are significantly more stable.[138] More generally, it appears to be crucial to determine whether the deactivation process is an intrinsic feature of the photocatalytic system or is specifically due to the use of a sacrificial electron donor generating potentially damaging radical species. The fact that a mixture of dyes **PS10b**,**c** and TEOA rapidly bleach in the absence of catalyst supports the latter hypothesis.[142]

3.4. Mechanisms

A first mechanistic issue regards whether reduction of the cobalt center occurs by direct oxidative quenching of the excited photosensitizer PS* or by reaction with the reduced photosensitizer PS^-, derived from a reductive quenching process of PS* by the sacrificial electron donor.

Photophysical studies have been carried out so as to adress this issue. Ruthenium–diimine photosensitizers, such as **PS1** or **PS2**, absorb visible photons at around 450 nm, which promote one electron from the metal d orbitals to the antibonding π orbital of a diimine ligand. The excited state formed immediately upon excitation with a $S = 0$ spin configuration (singlet) rapidly converts into a triplet state ($S = 1$) though a mechanism called intersystem crossing and involving spin–orbit coupling. This yields an excited state PS* (Figure 16) with quite a long lifetime (a few μs) that can be described as a Ru^{III} center coordinated to a reduced diimine radical anion ligand.[156] Because of the presence of an electron in the π^* orbital of a bipy ligand, this excited state is a quite powerful reducing agent, with a standard potential of −0.86 V vs NHE in the case of **PS1**. At the same time, and owing to the presence of an unoccupied d orbital at the metal center, PS* can also act as a powerful oxidizing species with $E° = 0.84$ V versus NHE in the case of **PS1**.[157] The nature and concentration of redox partners then essentially control the reactivity of PS* as either a reducing or oxidizing species. Different systems are discussed below.

When $[Co(bipy)_3]^{2+}$ is used as the catalyst and ascorbate employed as the sacrificial electron donor in a photochemical H_2-evolving system, PS* (**PS1** or **PS2**) is first reduced by ascorbate into PS^- (reductive quenching; Figure 16). In the presence of TEOA however, oxidative quenching (Figure 16) yielding $[Co(bpy)_3]^+$ is faster than conversion of PS* into PS^-.[57,60,128]

With cobaloxime as a catalyst, a reductive quenching process dominates in the presence of TEOA. In the case of H-bridged cobaloximes, this observation is consistent with the quite negative Co^{II}/Co^I redox potential.[131] Transient optical spectroscopic measurements[100,152] performed on the supramolecular assemblies **41a**, **49**, and **50**, containing a BF_2-annulated cobaloxime, show only a slight effect of the Co center on the Ru^{II} MLCT excited-state lifetime, confirming that reductive quenching by the sacrificial electron donor is the major pathway. In contrast, oxidative quenching is possible when the catalytic center is in the Co^{III} state.[100,152]

Similar studies have been carried out with other photosensitizers. For example, diffusion-controlled reductive

quenching operates in the case of rhenium-based photosensitizers, such as **PS5b,c**,[152] whereas oxidative quenching is evidenced in the case of platinum-based sensitizers, such as **PS6a**.[152] Finally, with iridium-based **PS3** and **PS4** photosensitizers, both mechanisms can operate depending on the relative concentrations of the catalyst and the electron donor.[133]

Electron transfers from organic dyes were also examined by fluorescence spectroscopy and laser flash photolysis techniques. For xanthene dyes **PS8** and **PS9**, the electron transfer to cobaloxime (either Co^{II} or Co^{III} states) was found to occur from the triplet state.[136,141] Both oxidative and reductive quenching mechanisms may contribute to catalysis. In contrast, the Co^{III} clathrochelate complexes **28** and **29** can oxidatively quench both the singlet and triplet excited states of **PS9**.[136] No oxidative quenching of the excited state of the perylene-3,4:9,10-bis(dicarboximide) moiety by the Co^{II} center could be seen in **51**, but this might be due to the large extent of dissociation of this compound in solution.[152]

A second important issue regards the mechanism of H_2 formation. In the polypyridine–cobalt series, the major cobalt(II) complexes formed in solution are the bipyridine species $[Co(bipy)_n]^{2+}$ ($n=1$ and 2). Generation of cobalt(I) complexes under irradiation is seen by the blue color of the solution, and dissociation of bipy ligands from $[Co^{I}(bipy)_3]^{+}$ has been evidenced under catalytically relevant conditions.[58] In fact, the hydride complex **22**, independently prepared by pulse radiolysis of aqueous $CoSO_4$–bipy mixtures in the presence of radical scavengers,[59] is likely to be the key catalytic intermediate during hydrogen photogeneration from aqueous solutions.[57,60]

Formation of a Co^{I} species has been also observed using spectroscopy during reactions involving cobaloxime catalyts in combination with platinum sensitizers[117] or organic dyes in solution.[136] From photogenerated Co^{I} species, protonation yields Co^{III}-hydride species. At that stage, three different pathways can operate to liberate H_2 and close the cycle. First, the Co^{III}-hydride can directly react with a proton to liberate H_2 via a heterolytic pathway, followed by a reduction step yielding the Co^{II} species (heterolytic path A in Figure 13). Second, as proposed for the BF_2-annulated cobaloxime **9**, reduction of the Co^{III} hydride to the Co^{II} hydride complex proceeds before heterolytic reaction with a proton, liberating H_2 (heterolytic path B in Figure 13).[52,101] In both mechanisms, an extra electron is thus required, which can arise either from a second light-driven cycle or from a dark transfer process, that is, degradation of the radical cation $D^{\bullet+}$, which furnishes one equivalent of proton and one equivalent of electron (Figure 16). The third pathway is homolytic in nature, with hydrogen evolution resulting from the reductive elimination from either two Co^{III} hydride or two Co^{II} hydride species (homolytic path A and B in Figure 13).

During the course of a light-driven H_2 production catalysed by **PS5b** and **11**, Alberto and co-workers observed a quadratic dependence of the rate of H_2 evolution as a function of the total concentration of cobalt catalyst. This indicates a second-order process in cobalt as the rate-determining step and would be consistent with a homolytic mechanism. Other systems however display a linear dependence of the rate of H_2 production with respect to Co concentration.[117,135] In that case, it is very difficult to conclude for a heterolytic cobalt-centered H_2-evolving step, as other first-order processes in cobalt, such as electron transfer from the photosensitizer to the cobalt center, appear in the overall mechanism (Figure 15) and may also be rate-determining.[158]

In conclusion, cobaloxime complexes, unlike $[Co(bipy)_3]^{2+}$, are not very efficient quenchers of excited states of metal–diimine photosensitizers, and most light-driven H_2-evolving processes catalyzed by cobaloximes depend on a first reductive quenching step involving the sacrificial electron donor. Exceptions to this rule are found when organic dyes of the xanthene series are used.[136,141,142] Furthermore, the latter systems only contain earth-abundant elements. They thus appear as good candidates for the construction of H_2-evolving photocathode materials through their grafting onto transparent conductive materials.

4. Electrode Materials

A number of groups have extended their studies of H_2-evolving metal catalysts (Section 2) to their immobilization on surfaces and characterization of the systems thus formed with the objective of designing cheap and robust carbon-based electrodes for H_2 production.

Covalent grafting appears to be the method of choice for the design of stable electrocatalytic materials.[84,159] Spiro et al. initially reported covalent grafting of a cobalt *meso*-tetrakis(2-aminophenyl)porphyrin on glassy carbon electrodes by an amide link with carboxylic acid surface groups. These electrodes displayed high activity for H_2 production at a low overpotential (200 mV) in neutral aqueous solution (phosphate buffer) but were found quite fragile upon cycling, indicating that the attachment is not stable under the catalytic conditions.[160] Peters grafted the bis(imine-oxime) complex **20a** via the formation of inorganic ester linkages between the carboxylic groups of the ligands and surface metal-hydroxyl functions of an ITO electrode. Surface coverage was estimated to roughly correspond to a monolayer. However no clear evidence was given about the gain in electrocatalytic performances as compared to bare ITO electrodes under similar conditions. Furthermore leaching of the catalyst is observed over hours.[56]

Alternatively, thick electroactive films were obtained by copolymerization of the cobalt complex **7** with *p*-xylyl-α-α′-dibromide to form a cross-linked pyridinium-based polycation. A solution of the polymer in $CHCl_3$/ethanol solution was deposited on a glassy carbon electrode and evaporated. The resulting film shows catalytic H_2 evolution activity but the cathodic current decreased upon successive scans. Disrupting processes (with H_2 bubble formation) or chemical alteration at the film–electrode interface that would inhibit electron transfer between the electrode and the catalyst were postulated, because spectroscopic measurements carried out before and after catalysis did not reveal any leaching or degradation of the catalyst. Similar results were obtained with cobalt protoporphyrin films obtained by electropolymerization at

the surface by the electro-oxidation of peripheral vinyl substituents.[160]

Spiro et al. reported that stable catalytic materials can be simply obtained by incorporating positively charged cobalt porphyrin complexes **6** and **8** (Figure 2) into a Nafion film laid onto a glassy carbon electrode. However, a low electroactivity was observed in 0.1 mol L^{-1} aqueous TFA solution (26 turnovers achieved after 90 min at −0.95 V versus SCE when **6** is used as the catalyt), because of the poor electron-transfer characteristics of Nafion films.[160] When coated on a bare pyrolytic graphite electrode neutral, [Co(TPP)] (Figure 2) incorporated in a Nafion film can reduce protons, but only with a large overpotential (−0.7 V versus Ag/AgCl; pH 1) and a quite low 70 h^{-1} turnover frequency value.[70] Better catalytic activity (TOF 2×10^5 h^{-1}) was observed with an applied potential of −0.90 V vs Ag/AgCl and at pH 1 for cobalt phthalocyanine **52a** (Figure 23) incorporated in a poly(4-vinylpyridine-*co*-styrene) film deposited on a graphite electrode.[71] Other derivatives **52b** and **52c** were shown to be less active under similar conditions. Here again the catalytic proton reduction was limited by the electron transfer within the matrix.

A very active electrode material was obtained when GC electrodes were cycled (or poised) at a negative potential in a CH_3CN solution containing cobaloxime **9** and 0.05 mol L^{-1} solutions of *p*-toluenesulfonic acid.[56] The resulting modified electrode shows high catalytic currents corresponding to H_2 evolution from aqueous solutions (pH 2–7) with low overvoltages. Mixing **9** with black carbon and Nafion also yields an electroactive material that evolves H_2 from aqueous sulfuric acid solutions with onset potential as low as −0.45 V vs SCE.[54] However in these two examples, there is no evidence for a conserved integrity of **9** within the modified electrode materials during catalysis. Electrochemical deposition of metallic cobalt or cobalt oxide/hydroxide on electrode surfaces is a well-known process that could occur under these circumstances, and electrodeposited cobalt coatings are known to catalyze H_2 evolution at potentials similar to that reported for electrodes obtained from **9**.[161]

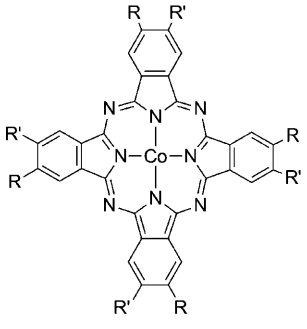

Figure 23. Structures of cobalt phthalocyanine complexes incorporated into polymer films and deposited onto electrode surfaces.

5. Cobalt Catalysts for Water Oxidation

As discussed above, the need to find new economically viable materials for water oxidation also excludes the development of noble metals (Pt, Pt/Ru) and noble metal oxides (RuO_2 or IrO_2),[162–165] even though such materials, with an overpotential requirement not exceeding 150–200 mV under acidic conditions, are the most active catalysts to date.[166] In naturally occurring systems, a first-row transition metal, manganese, achieves water oxidation catalysis at neutral pH. The oxygen-evolving center in photosystem II contains a mixture of manganese and calcium ions in a $CaMn_4$ stoichiometry, consisting of a $CaMn_3$ cubane arrangement, where ions are bridged by oxo groups, with a fourth manganese ion linked to this cluster.[4,167]

Recently, great achievements have been made regarding manganese- and ruthenium-based homogeneous molecular coordination compounds[41,43,159,168] as catalysts for water oxidation: the first report by Meyer and co-workers was on the so-called "blue dimer", a binuclear oxo-bridged ruthenium complex.[169] However, all of these compounds contain organic ligands that are thermodynamically unstable under the highly oxidizing conditions of the reaction and thus suffer from extensive oxidative degradation. As a consequence, most of these catalysts reported to date are oxidatively deactivated during reaction and function only during very short time periods. Nevertheless, these compounds provide unique tools to understand the chemistry of the oxygen-evolving process at work in biological photosystems. However, at present they do not appear to be competitive with to the more robust and active heterogeneous oxide materials. Exceptions recently appeared in the literature with polyoxometallate compounds containing active sites for water-oxidation catalysis embedded into a fully inorganic framework resistant to oxidative corrosion.[39,40,170,171] At the same time, there has been a renewed interest regarding solid metal oxide/hydroxide materials and nanomaterials as promising water oxidation catalysts and their further implementation into light-driven systems.

5.1. Co^{III}/Co^{II}: A Redox Couple for Water Oxidation

The competence of cobalt complexes for catalytic oxygen evolution from water was recognized long ago.[172] On the basis of standard potentials of the $[M(H_2O)_6]^{3+}/(M(H_2O)_6]^{2+}$ redox couple in the first-row transition-metal series, cobalt provides the most oxidizing system ($E^0 = 1.84$ V vs NHE, acidic solution) before manganese (1.59 V vs NHE) and iron (0.77 V vs NHE). As a consequence, in the absence of ligands that stabilize Co^{III}, oxidation of Co^{II} is very unfavorable and Co^{III} is reduced by water. It is tempting to suggest that manganese was preferred to cobalt at the catalytic site of photosystem II, not only because of the lowest abundance of cobalt in the earth crust, but also because the redox potentials of high-valent cobalt species lie too high above that of water oxidation.

Seminal papers on cobalt-catalyzed water oxidation appeared in the 70s and 80s that showed that Co^{II} salts are

able to catalyze the oxidation of water by permanganate,[173,174] hypochlorite,[175] persulfate,[175] perruthenate, and ferrate,[174] and also $[IrCl_6]^{2-}$ and $(Ru(bipy)_3)^{3+}$ complexes.[176] In 1967, Anbar and Pecht proposed a mechanism for water oxidation in acidic to neutral solution that involved a bis(μ-hydroxo)dicobalt(III) species. $HO_2^{\bullet}$ radicals are generated from this dimeric species through an inner-sphere process and then O_2 is generated.[177] In 1978, Shafirovich et al. showed for the first time that Co^{II} ions could behave as electrocatalysts for the oxidation of water at basic to neutral pH.[178] Since the catalytic wave was observed at considerably more negative potentials (0.9–1 V vs SCE at pH 10) than that of the Co^{III}/Co^{II} couple (1.6 V vs SCE) and at basic pH values, it was concluded that the active catalyst was a cobalt hydroxo species adsorbing onto the surface of the electrode so that the electrocatalytic wave is a mixed "volume"–"surface" response. In this system, electrochemical oxidation of Co^{II} was supposed to generate high-valent Co^{IV} hydroxo complexes responsible for the bielectronic oxidation of water to hydrogen peroxide, which eventually decomposes into oxygen (Figure 24) and water. Co^{II} is regenerated during the H_2O_2 formation step. The mechanism shown in Figure 24 was established by Sutin et al. in 1983 from kinetic studies of the Co^{II}-catalyzed oxidation of water by $[Ru(bpy)_3]^{3+}$.[179] The rate constant for the reaction of Co^{IV} with water or hydroxide ions was estimated to be $100\ s^{-1}$. However, mechanistic details of the O–O bond formation reaction at Co^{IV} still have not been obtained.

$$Co^{2+} + 2\,H_2O \rightleftharpoons Co(OH)_2 + 2\,H^+$$

$$Co(OH)_2 \rightleftharpoons Co(OH)_2^+ + e^-$$

$$Co(OH)_2^+ \rightleftharpoons CoO^{2+} + H_2O + e^-$$

$$CoO^{2+} + H_2O \rightleftharpoons Co^{2+} + H_2O_2$$

Figure 24. Mechanism established from kinetic studies for the Co^{II}-catalyzed oxidation of water in basic solution. $[Ru(bpy)_3]^{3+}$ is acting as the oxidizing species.

Recently, Hill and co-workers described the catalytic activity for water oxidation of the homogeneous polyoxometalate inorganic compound $[Co_4(H_2O)_2\{\alpha\text{-}PW_9O_{34}\}_2]^{10-}$ that contains an active Co_4 core (Figure 25).[180] This complex, initially prepared in 1973,[181] is free of carbon-based organic ligands and is thus expected to be resistant to oxidation. Cyclic voltammetry of $[Co_4(H_2O)_2(\alpha\text{-}PW_9O_{34})_2]^{10-}$ shows a large catalytic current with a low overpotential for water oxidation ($E = 1.1$ V vs Ag/AgCl, pH 8). Using $[Ru(bpy)_3]^{3+}$ as the oxidant, O_2 evolution from water (pH 8) was observed (60% yield, 75 turnovers, TOF = $5\ s^{-1}$). The reaction is limited in part by oxidation of the bipyridine ligand. With a large concentration of the oxidant ($2.4\ mmol\,L^{-1}$) and $0.12\ \mu mol\,L^{-1}$ catalyst, a turnover number of 1000 was obtained in 3 min. The authors provide several points of evidence that the observed activity is not driven from Co ions or/and Co hydroxide/oxide species released from the polyoxometalate as the result of oxidative degradation.

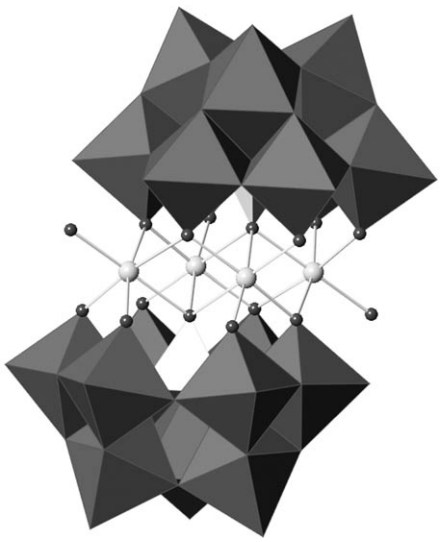

Figure 25. Structure of $[Co_4(H_2O)_2\{\alpha\text{-}PW_9O_{34}\}_2]^{10-}$. The $\{\alpha\text{-}PW_9O_{34}\}$ subunits are represented as polyhedra with dark gray $\{WO_6\}$ octahedra and light gray $\{PO_4\}$ tetrahedra. Cobalt ions: gray spheres, oxygen atoms coordinated to cobalt: dark gray spheres.

5.2. Cobalt Oxides

There have been many reports in the literature concerning the use of cobalt oxide/hydroxide materials as electrode coatings that catalyze water oxidation. Various methods of preparation from soluble Co^{II} salts (anodic deposition in alkaline[161,182–185] or acidic to neutral[186,187] solution, cathodic deposition from $CoCl_2$,[188–196] possibly in the presence of acetate anions,[197,198] passivation of a cobalt electrode,[199] chemical vapour deposition,[200] or reactive sputtering in O_2 plasma[201]) have been described and these result in distinct stoichiometries. The activity of cubic Co_3O_4 nanoparticles has also been reported.[202,203] All of these compounds are typically assayed as catalytic coatings for water oxidation and require overpotentials in the 200–400 mV range[204] in strongly alkaline aqueous solution where they are more stable than noble metal oxides. Several distinct mechanisms have been proposed to account for such a catalytic activity.[199,205] Recently however, this field of research experienced a burst of interest, and the possibility of using such cobalt oxide coatings to catalyze water oxidation in neutral aqueous solutions has now been extensively reconsidered.

Oxidation of aqueous Co^{II} was reinvestigated by Nocera in 2008. Controlled potential electrolysis of Co^{II} salts in pH 7 phosphate (P_i) buffer at 1.3 V vs NHE resulted in the deposition of an amorphous Co^{III} oxide/hydroxide precipitate.[206,207] This precipitation occurs at the surface of different conducting materials (such as ITO, FTO (F:SnO_2), or glassy carbon). The deposit is resistant to dehydration and the effects of air exposure and mechanical treatment. The absence of crystalline features in the powder X-ray diffraction pattern and diffraction patterns in the TEM indicates that the active unit is less than 5 nm in size and thus of molecular nature.[207] The nuclearity of the clusters in the material depends on the thickness of the deposit.[208] Chemical analysis

and X-ray absorption spectroscopy were in good agreement with Co atoms, which are predominantly in an octahedral configuration with 6 oxygen ligands (d(Co–O) = 1.89 Å, d(Co–Co) = 2.8 Å). Two non-exclusive structures have been proposed for the molecular clusters at the surface and/or in the bulk material (Figure 26). The first consists of interconnected Co^{III}–oxo/hydroxo cubanes, with complete or incomplete cubanes sharing a Co corner.[208–210] The second is based on edge-sharing CoO_6 octahedra in Co–oxo/hydroxo incomplete cubane cluster forming tile-shaped units whose structure is analogous to that of alkali metal cobaltate.[208] Phosphate ions may be present as terminal, but not bridging, ligand to cobalt centers.[209]

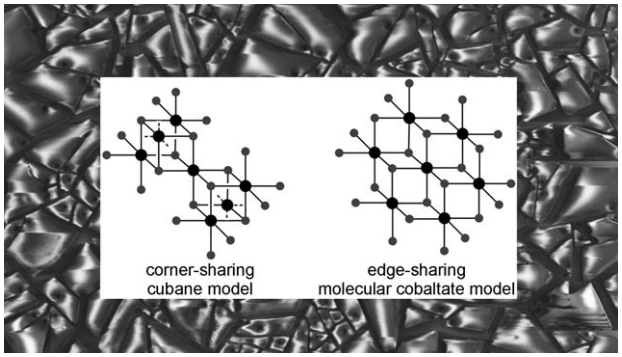

Figure 26. Scanning electron micrograph of a film obtained by the method reported by Nocera and proposed structural motif deduced from XAS data relating to the bulk of this catalytic film material. Cobalt ions: black spheres, oxygen atoms: gray spheres.

Films with similar structure and compositions are formed when sputter-deposited thin films (800 nm thick) of cobalt metal are anodized in a phosphate electrolyte, thereby indicating similarities between surface metal oxide coatings obtained upon passivation of cobalt electrodes and bulk metal oxide films deposited from Co^{II} solutions.[211]

The obtained solid material was shown to be catalytically active for the electrooxidation of neutral pH (phosphate buffer) water in the absence of Co^{II} ions in solution. Indeed, electrolysis at 1.3 V vs NHE (0.5 V overpotential) resulted in the formation of O_2, which is derived from water as shown from labeling experiments and mass spectrometry, with a Faradaic efficiency close to 100 % and current densities in the order of 1–10 mA cm^{-2}. A current density of 1 mA cm^{-2} requires an overvoltage of 0.4 V; turnover frequencies of 0.001 s^{-1} can be estimated. Under such neutral conditions, this catalyst oxidizes water preferentially to chloride ions.[207] Similar catalytic films can be electrodeposited from pH 8.5 methylphosphonate and pH 9.2 borate electrolytes. These thicker coatings achieve a higher current density of 100 mA cm^{-2} for water oxidation at 442 and 363 mV overpotential, respectively.[212]

The mechanism of water oxidation catalyzed by Co-oxo/hydroxo species shown in Figure 23 also applies to the system described here. Formation of the catalytic film results from oxidation of Co^{II} to Co^{III}, which as expected precipitates on the surface of the electrode in the presence of phosphate. Further oxidation generates Co^{IV} oxo species from which O_2 is produced.[213] In this last reaction step, Co^{II} is regenerated. EPR spectroscopy provided clear evidence for the formation of Co^{IV} species during electrocatalytic water oxidation.[214] XAS measurements are also consistent with a valency for cobalt of greater than 3.[208] Importantly, the film undergoes continual reduction (associated with O_2 evolution) upon switching to an open circuit from 1.25 V vs NHE. This property is related to the molecular nature of the film: by comparison, solid-state cobaltate materials with similar high cobalt valencies are kinetically stable to water under similar conditions. The overall mechanism involves proton-coupled electron-transfer steps before the generally rate-determining O_2 evolution step. Indeed it is likely that O–O bond formation requires the corresponding molecules of water or hydroxide anions to be activated by deprotonation. It has been suggested that phosphate ions, acting as proton acceptors, play a major role in this process.[213]

Another function of phosphate ions resides in their ability to continuously reintegrate solubilized Co^{II} ions into the film during catalysis through precipitation of Co^{III} ions.[215,216] Indeed, during turnover or when the electrode is held at open circuit potential, Co^{II}, a substitutionally labile high-spin ion in an oxygen environment, returns to the solution (dissolution of the oxide); however, under oxidizing conditions and in the presence of phosphate, the substitutionally inert low-spin d^6 Co^{III} ion is immediately deposited back at the surface of the electrode. This repair process and the role of phosphate ions have been well-established using films labeled with radioactive ^{57}Co and ^{32}P and monitoring release/uptake of the isotopes during water oxidation catalysis.[215]

This metal oxide is one of the rare examples for which activity at neutral pH is demonstrated. In fact, a cobalt oxide material of composition $CoO_m{\cdot}n\,H_2O$ (with m = 1.4–1.7 and n = 0.1–1) was reported in 1964.[186] This compound was formed by anodic deposition of a cobalt salt, such as nitrate, sulphate, acetate, and fluoroborate, at 0.7 V vs SCE in aqueous solution (pH 6 or 7). This material is described as being stable at a pH above 1 in solutions containing chloride, sulphate, or nitrate ions and catalyzes water oxidation in 0.5 mol L^{-1} K_2SO_4 solution at 1.43 V vs SCE. More recently, Stahl and co-workers deposited a fluoride-containing cobalt oxide on a FTO electrode from $CoSO_4$ solution (pH 3.5) in the presence of fluoride anions.[217] This compound was found to be active for sustained water oxidation at 1.6 V vs NHE from solutions of initial pH 3.7 in the presence of fluoride anions and stable for pH > 3. The current density (ca. 2 to 6 mA cm^{-2}) observed at the electrode increases with the concentration of fluoride in solution (0.1 to 1 mmol L^{-1}). Fluoride anions were thus proposed to act as proton acceptors, in the same way as phosphate anions do in Nocera's studies.[218] This material does not differ much from those obtained by the groups of Nocera[207] or Chen and Noufi[187] in terms of the overpotential for O_2 evolution. However, distinct current densities are observed that result from different thicknesses of the electrodeposited material and/or different conductivities of the coatings. A strong dependence of current densities with the nature of the electrolyte (F^- or P_i) is noted and rationalized in terms of electrolyte competing with water for coordination to cobalt during turnover.

5.3. Photochemical Water Oxidation: From Homogeneous Systems to Photoanode Materials

5.3.1. Soluble Systems and Particles

The use of cobalt salts to catalyze light-driven water oxidation was initially investigated by Shafirovich et al. in 1980.[176] Irradiation of a phosphate-buffered (pH 5–7) aqueous solution of $[Ru(bipy)_3]^{2+}$ and $[Co(NH_3)_5Cl]$ generates low yields of O_2. It is proposed that hydrolysis of $[Co(NH_3)_5Cl]$ liberates Co^{II} ions, which then behave as precursors of the active species. Addition of $CoSO_4$ into the photolysis solution indeed increases the yield for O_2 evolution significantly.[219] A quantum efficiency of 12% could be measured. This system was studied by Sutin and co-workers to further characterize the reaction mechanism, but the nature of the catalyst remains undefined.[179] Recently, Styring and co-workers observed that a colloidal catalyst with spherical nanoparticules (10–60 nm radius) is produced when methylenediphosphonate is added to the photolyzed solution. Oxygen (TON $\approx$ 20) is produced in aqueous solution at pH 7 under visible irradiation with $[Ru(bipy)_3]^{2+}$ as the photosensitizer and peroxodisulfate as the electron acceptor.[220]

Harriman and co-workers investigated a combination of various dispersed powders of metal oxides with $[Ru(bipy)_3]^{2+}$ as the photosensitizer and peroxodisulfate as the electron acceptor for light-driven water oxidation in deaerated aqueous $NaSO_4$ solution (pH 5).[221] The spinels $NiCo_2O_4$ and Co_3O_4 were found to be quite active under these conditions, with Co_3O_4 ranking just below the species IrO_2 and above RuO_2.

A similar system was recently reported by the group of Frei using cobalt oxide nanoparticles deposited on silica.[222] By using wet impregnation of SBA-15 silica by $Co(NO_3)_2$ in ethanol followed by controlled calcination, cobalt oxide nanoclusters could be formed in the mesopores of silica. Structural characterization reveals spheroid-shaped bundles (bundle diameter 35 nm) of parallel Co_3O_4 nanorods (8 nm diameter, 50 nm length, 14 nanorods per bundle) of spinel structure inside the porous silica scaffold, interconnected by short bridges. Suspensions of the silica particles containing Co_3O_4 clusters (4% loading) in pH 5.8 aqueous solution were able to oxidize water to O_2 upon visible light illumination in the presence of $[Ru(bipy)_3]^{2+}$ as a photosensitizer and peroxodisulfate as the electron acceptor. A 18% quantum efficiency was reported. Remarkable TOF values in the range of 1000 s^{-1} per nanocluster were observed, which are about three orders of magnitude greater than those observed using micrometer-sized Co_3O_4 particles as a consequence of both the larger surface area derived from the nanostructuring of the material and the higher activity of Co surface sites (TOF = 0.01 s^{-1} per surface Co site).

The polyoxometallate $[Co_4(H_2O)_2\{\alpha\text{-}PW_9O_{34}\}_2]^{10-}$ (Figure 25) combined with $[Ru(bipy)_3]^{2+}$ also proved active in the course of oxygen photoproduction at pH 8 with peroxodisulfate as the electron acceptor. Quantum yields of 30% and turnover number of more than 220 were obtained.[223]

It should be noted that the experimental conditions used for such photocatalytic assays should be controlled precisely, in particular by well-defined control experiments. For example, Collomb and co-workers observed that O_2 is produced from irradiated pH 3 aqueous solutions of $[Ru(bipy)_3]^{2+}$ and peroxodisulfate in the absence of any catalyst.[224] In that case, a chloroacetate buffer was used. The pH of the solution may thus play an important role. Furthermore, aqueous solutions of $S_2O_8^{2-}$ are decomposed under UV irradiation to produce O_2.[225]

5.3.2. Cobalt-Based Photoanodes for O_2 Evolution

There are only very few photoanodes that are based on cobalt compounds. One is the ITO-PTCBI-**52a** electrode, with the n-type organic semiconductor PTCBI (3,4,9,10-perylenetetracarboxylic acid bisbenzimidazole; Figure 27). This electrode consists of a layer of the semiconductor on an ITO-coated glass, covered with a second layer of **52a** acting as a catalyst. Using this organic photoanode coupled to a platinum counter electrode, a continuous water splitting to O_2 and H_2 was observed (pH 11) under exposure to visible light. Using a bias potential of 0.4 V vs Ag/AgCl, the reaction yielded 3500 turnovers per hour. It thus appears that this stable PTCBI-**52a** bilayer, which exploits the capacity of the Co^{III}–phthtalocyanine complex to oxidize water to O_2, could constitute an interesting material for an artificial photosynthetic system.

Cobalt compounds have been also used to enhance the catalytic efficiency of O_2-evolving photoanodes of photoelectrochemical cells, in which the external power required to

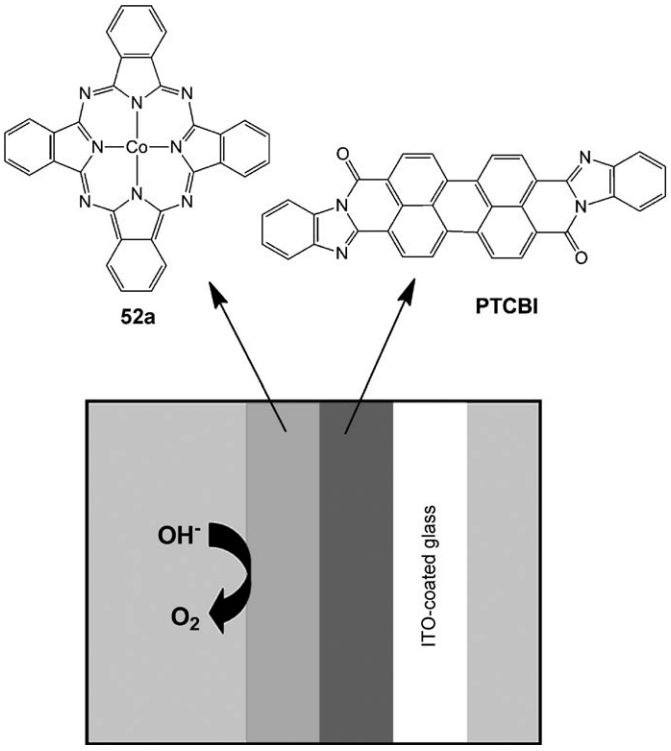

Figure 27. Structure of the perylene derivative/cobalt phthalocyanine **52a** bilayer photoanode for the photocatalytic oxidation of water described by Abe et al.[226]

drive the electrocatalyst derives at least partly from a light-harvesting semiconductor substrate. To optimize the utilization of incident light, catalysts for water oxidation should combine high turnover frequencies (on the order of 10 s^{-1}) and high surface densities (on the order of 10 catalytic sites per square nanometer) to achieve an ideal surfacic TOF of about 100 $s^{-1} nm^{-2}$.[204] Grätzel and co-workers initially demonstrated that a simple impregnation with cobalt nitrate of thin films of Si-doped α-Fe_2O_3 obtained from atmospheric-pressure chemical vapor deposition resulted in a 80 mV cathodic shift of the voltametric curve determined under irradiation, accompanied by a small increase of the photocurrent.[227] Thus adsorption of cobalt ions at the surface of hematite allows a 80 mV reduction of the overpotential for water photooxidation. The latter is however still quite high (ca. 1 V), as the onset of the wave observed under irradiation is at 0.9 V vs NHE in 1M NaOH solution.

The catalytic film material described by Nocera and co-workers has been recently exploited in composite photoanodes. It was shown to greatly enhance the efficiency of photoelectrochemical water oxidation when deposited on mesostructured α-Fe_2O_3[228,229] and ZnO[230] photoanodes. In the first case, it resulted in a 500 mV cathodic shift of the onset potential for water oxidation to O_2, at pH 8, and greatly increased incident photon-to-current efficiencies.[228,229] Thus integration of cobalt oxide film with α-Fe_2O_3 provides a substantial reduction in the power needed to drive catalysis. In the second case, deposition of cobalt oxide was achieved photochemically. Photogenerated holes in a semiconductor, such as n-type ZnO, have been used to oxidize Co^{II} to Co^{III} to precipitate cobalt oxide at the surface.[230] By doing so, photodeposition places the cobalt oxide material at the location where the holes are most readily available, namely exactly where O_2 evolution is the most effective. The advantage over electrodeposition is enhanced O_2 evolution with less catalyst. The new composite photoanode displayed slightly increased photocurrent and overpotential for water photooxidation decreased by 0.2 V. Other composite photoanodes relying on CdS, TiO_2 and $GaInP_2$ semiconductors, the latter in tandem configuration with a p,n-GaAs photovoltaic device, have also been described by Nocera and co-workers.[231]

6. Summary and Outlook

Cobalt compounds, either as molecular species or three-dimensional materials, thus appear to be appealing multi-electron catalysts for both reductive (hydrogen production) and oxidative reactions (oxygen production) for the water-splitting process. However, to implement these compounds into practical industrial devices, there are some critical issues to address.

First, high stabilities of catalysts over cycling should not be restricted to neutral conditions, because industrial processes developed for electrolysis are generally run under strongly acidic or alkaline conditions. The stability of photosensitizers must also be improved before considering possible technological transfer. Detailed studies regarding the origin and the mechanisms of catalyst/photosensitizer decomposition reactions are of critical importance in that respect.

Second, soluble molecular active compounds have to be converted into electrode materials by efficient and cheap methods for grafting them on solid surfaces.[146] It is interesting to note that immobilization of molecular catalysts on nanostructured electrode surfaces might result in increased stability and sometimes increased activity.[84] This is true also for photosensitizers, as demonstrated in the case of ruthenium dyes and TiO_2 in dye-sensitized solar cells.[232]

Third, catalysts have to be coupled to photosensitizers. This has recently led to the development of new light-driven systems for H_2 or O_2 evolution. However these systems are generally assayed in homogeneous solution in the presence of sacrificial electron donors or acceptors. McDaniel and Bernhard recently proposed calculating the power efficiency of such systems as a figure of merit.[233] Such a computation is far from being easy and reliable because it requires the knowledge of thermodynamic data, such as redox potentials, which are difficult to determine in the solvent mixtures commonly used for photocatalysis experiments. Even though such studies facilitate understanding how catalyst–photosensitizer combinations function (factors such as kinetics and mechanisms), we believe that it is premature to consider such homogeneous systems as energy storage devices. In some cases indeed the experimental conditions do not result in net energy storage.[234] For example, the $S_2O_8^{2-}/SO_4^{2-}$ couple used in light-driven O_2 evolution assays has a potential near 2 V and is thus by itself capable from a thermodynamic standpoint to oxidize water.[235]

Fourth, in most studies, photocatalysis is limited by the photon flux. Comparison of different systems studied under different irradiation conditions thus requires them to be carefully characterized in terms of quantum yield and quantum efficiency, which is not always the case.

Implementation of such photocatalytic systems into molecularly engineered photoelectrode materials remains to be achieved, but the field is now mature, so that it is very likely that a fully molecular photoelectrocatalytic system for overall water splitting will appear in the very next future. The challenge now resides in the determination of the experimental conditions suitable for the concomitant operation of water-oxidizing and water-reducing (photo)catalytic systems.[236]

The authors thank the undergraduate and graduate students, post-docs, and young researchers from the group that all contributed to the development of this review. Eugen S. Andreiadis is especially acknowledged for the preparation of the frontispiece picture.

Received: December 17, 2010
Published online: July 11, 2011

[1] N. S. Lewis, D. G. Nocera, *Proc. Natl. Acad. Sci. USA* **2007**, *104*, 20142.
[2] T. R. Cook, D. K. Dogutan, S. Y. Reece, Y. Surendranath, T. S. Teets, D. G. Nocera, *Chem. Rev.* **2010**, *110*, 6474–6502.

[3] R. B. Gordon, M. Bertram, T. E. Graedel, *Proc. Natl. Acad. Sci. USA* **2006**, *103*, 1209 – 1214.
[4] Y. Umena, K. Kawakami, J. R. Shen, N. Kamiya, *Nature* **2011**, *473*, 55 – 65.
[5] A. Melis, L. P. Zhang, M. Forestier, M. L. Ghirardi, M. Seibert, *Plant Physiol.* **2000**, *122*, 127 – 135.
[6] A. Melis, T. Happe, *Plant Physiol.* **2001**, *127*, 740 – 748.
[7] M. L. Ghirardi, J. P. Zhang, J. W. Lee, T. Flynn, M. Seibert, E. Greenbaum, A. Melis, *Trends Biotechnol.* **2000**, *18*, 506 – 511.
[8] S. T. Stripp, T. Happe, *Dalton Trans.* **2009**, 9960 – 9969.
[9] A. C. Benniston, A. Harriman, *Mater. Today* **2008**, *11*, 26 – 34.
[10] D. Gust, D. Kramer, A. Moore, T. A. Moore, W. Vermaas, *MRS Bull.* **2008**, *33*, 383 – 387.
[11] J. Barber, *Chem. Soc. Rev.* **2009**, *38*, 185 – 196.
[12] J. C. Fontecilla-Camps, A. Volbeda, C. Cavazza, Y. Nicolet, *Chem. Rev.* **2007**, *107*, 4273 – 4303.
[13] D. Gust, T. A. Moore, A. L. Moore, *Acc. Chem. Res.* **2001**, *34*, 40 – 48.
[14] S. Fukuzumi, *Phys. Chem. Chem. Phys.* **2008**, *10*, 2283 – 2297.
[15] N. Aratani, D. Kim, A. Osuka, *Acc. Chem. Res.* **2009**, *42*, 1922 – 1934.
[16] O. S. Wenger, *Coord. Chem. Rev.* **2009**, *253*, 1439 – 1457.
[17] B. Albinsson, J. Martensson, *J. Photochem. Photobiol. C* **2008**, *9*, 138 – 155.
[18] A. Harriman, J. P. Sauvage, *Chem. Soc. Rev.* **1996**, *25*, 41 – 48.
[19] L. Flamigni, J. P. Collin, J. P. Sauvage, *Acc. Chem. Res.* **2008**, *41*, 857 – 871.
[20] H. Dürr, S. Bossmann, *Acc. Chem. Res.* **2001**, *34*, 905 – 917.
[21] M. R. Wasielewski, *J. Org. Chem.* **2006**, *71*, 5051 – 5066.
[22] M. R. Wasielewski, *Acc. Chem. Res.* **2009**, *42*, 1910 – 1921.
[23] T. Hasobe, *Phys. Chem. Chem. Phys.* **2010**, *12*, 44 – 57.
[24] C. Tard, C. J. Pickett, *Chem. Rev.* **2009**, *109*, 2245 – 2274.
[25] S. Canaguier, V. Artero, M. Fontecave, *Dalton Trans.* **2008**, 315 – 325.
[26] Y. Oudart, V. Artero, J. Pécaut, C. Lebrun, M. Fontecave, *Eur. J. Inorg. Chem.* **2007**, 2613 – 2626.
[27] S. Canaguier, L. Vaccaro, V. Artero, R. Ostermann, J. Pécaut, M. J. Field, M. Fontecave, *Chem. Eur. J.* **2009**, *15*, 9350 – 9365.
[28] Y. Oudart, V. Artero, L. Norel, C. Train, J. Pécaut, M. Fontecave, *J. Organomet. Chem.* **2009**, *694*, 2866 – 2869.
[29] L. Vaccaro, V. Artero, S. Canaguier, M. Fontecave, M. J. Field, *Dalton Trans.* **2010**, *39*, 3043 – 3049.
[30] S. Canaguier, M. Fontecave, V. Artero, *Eur. J. Inorg. Chem.* **2011**, 1094 – 1099.
[31] V. Fourmond, S. Canaguier, B. Golly, M. J. Field, M. Fontecave, V. Artero, *Energy Environ. Sci.* **2011**, DOI: 10.1039/c1030ee00736f.
[32] B. E. Barton, C. M. Whaley, T. B. Rauchfuss, D. L. Gray, *J. Am. Chem. Soc.* **2009**, *131*, 6942 – 6943.
[33] S. Canaguier, M. Field, Y. Oudart, J. Pécaut, M. Fontecave, V. Artero, *Chem. Commun.* **2010**, *46*, 5876 – 5878.
[34] B. E. Barton, T. B. Rauchfuss, *J. Am. Chem. Soc.* **2010**, *132*, 14877 – 14885.
[35] R. Brimblecombe, G. F. Swiegers, G. C. Dismukes, L. Spiccia, *Angew. Chem.* **2008**, *120*, 7445 – 7448; *Angew. Chem. Int. Ed.* **2008**, *47*, 7335 – 7338.
[36] Y. H. Xu, T. Akermark, V. Gyollai, D. P. Zou, L. Eriksson, L. L. Duan, R. Zhang, B. Akermark, L. Sun, *Inorg. Chem.* **2009**, *48*, 2717 – 2719.
[37] L. Duan, Y. Xu, P. Zhang, M. Wang, L. Sun, *Inorg. Chem.* **2010**, *49*, 209 – 215.
[38] Y. Xu, A. Fischer, L. Duan, L. Tong, E. Gabrielsson, B. Åkermark, L. Sun, *Angew. Chem.* **2010**, *122*, 9118 – 9121; *Angew. Chem. Int. Ed.* **2010**, *49*, 8934 – 8937.
[39] Y. V. Geletii, B. Botar, P. Koegerler, D. A. Hillesheim, D. G. Musaev, C. L. Hill, *Angew. Chem.* **2008**, *120*, 3960 – 3963; *Angew. Chem. Int. Ed.* **2008**, *47*, 3896 – 3899.
[40] A. Sartorel, M. Carraro, G. Scorrano, R. De Zorzi, S. Geremia, N. D. McDaniel, S. Bernhard, M. Bonchio, *J. Am. Chem. Soc.* **2008**, *130*, 5006 – 5007.
[41] X. Sala, I. Romero, M. Rodriguez, L. Escriche, A. Llobet, *Angew. Chem.* **2009**, *121*, 2882 – 2893; *Angew. Chem. Int. Ed.* **2009**, *48*, 2842 – 2852.
[42] G. C. Dismukes, R. Brimblecombe, G. A. N. Felton, R. S. Pryadun, J. E. Sheats, L. Spiccia, G. F. Swiegers, *Acc. Chem. Res.* **2009**, *42*, 1935 – 1943.
[43] R. Brimblecombe, G. C. Dismukes, G. F. Swiegers, L. Spiccia, *Dalton Trans.* **2009**, 9374 – 9384.
[44] M. Wang, L. Sun, *ChemSusChem* **2010**, *3*, 551 – 554.
[45] V. Artero, M. Fontecave, *Coord. Chem. Rev.* **2005**, *249*, 1518 – 1535.
[46] S. Losse, J. G. Vos, S. Rau, *Coord. Chem. Rev.* **2010**, *254*, 2492 – 2504.
[47] B. Fisher, R. Eisenberg, *J. Am. Chem. Soc.* **1980**, *102*, 7361 – 7363.
[48] X. Hu, B. S. Brunschwig, J. C. Peters, *J. Am. Chem. Soc.* **2007**, *129*, 8988 – 8998.
[49] R. M. Kellett, T. G. Spiro, *Inorg. Chem.* **1985**, *24*, 2373 – 2377.
[50] P. Connolly, J. H. Espenson, *Inorg. Chem.* **1986**, *25*, 2684 – 2688.
[51] M. Razavet, V. Artero, M. Fontecave, *Inorg. Chem.* **2005**, *44*, 4786 – 4795.
[52] C. Baffert, V. Artero, M. Fontecave, *Inorg. Chem.* **2007**, *46*, 1817 – 1824.
[53] X. L. Hu, B. M. Cossairt, B. S. Brunschwig, N. S. Lewis, J. C. Peters, *Chem. Commun.* **2005**, 4723 – 4725.
[54] O. Pantani, E. Anxolabehere-Mallart, A. Aukauloo, P. Millet, *Electrochem. Commun.* **2007**, *9*, 54 – 58.
[55] P.-A. Jacques, V. Artero, J. Pécaut, M. Fontecave, *Proc. Natl. Acad. Sci. USA* **2009**, *106*, 20627 – 20632.
[56] L. A. Berben, J. C. Peters, *Chem. Commun.* **2010**, *46*, 398 – 400.
[57] C. V. Krishnan, B. S. Brunschwig, C. Creutz, N. Sutin, *J. Am. Chem. Soc.* **1985**, *107*, 2005 – 2015.
[58] H. A. Schwarz, C. Creutz, N. Sutin, *Inorg. Chem.* **1985**, *24*, 433 – 439.
[59] C. Creutz, H. A. Schwarz, N. Sutin, *J. Am. Chem. Soc.* **1984**, *106*, 3036 – 3037.
[60] C. Creutz, N. Sutin, *Coord. Chem. Rev.* **1985**, *64*, 321 – 341.
[61] J. P. Bigi, T. E. Hanna, W. H. Harman, A. Chang, C. J. Chang, *Chem. Commun.* **2010**, *46*, 958 – 960.
[62] P. V. Bernhardt, L. A. Jones, *Inorg. Chem.* **1999**, *38*, 5086 – 5090.
[63] V. Houlding, T. Geiger, U. Kölle, M. Grätzel, *J. Chem. Soc. Chem. Commun.* **1982**, 681 – 683.
[64] O. Pantani, S. Naskar, R. Guillot, P. Millet, E. Anxolabehere-Mallart, A. Aukauloo, *Angew. Chem.* **2008**, *120*, 10096 – 10098; *Angew. Chem. Int. Ed.* **2008**, *47*, 9948 – 9950.
[65] U. Kölle, S. Ohst, *Inorg. Chem.* **1986**, *25*, 2689 – 2694.
[66] U. Kölle, E. Raabe, C. Krüger, F. P. Rotzinger, *Chem. Ber.* **1987**, *120*, 979 – 985.
[67] G. M. Jacobsen, J. Y. Yang, B. Twamley, A. D. Wilson, R. M. Bullock, M. R. DuBois, D. L. DuBois, *Energy Environ. Sci.* **2008**, *1*, 167 – 174.
[68] E. S. Wiedner, J. Y. Yang, W. G. Dougherty, W. S. Kassel, R. M. Bullock, M. Rakowski DuBois, D. L. DuBois, *Organometallics* **2010**, *29*, 5390 – 5401.
[69] N. K. Szymczak, L. A. Berben, J. C. Peters, *Chem. Commun.* **2009**, 6729 – 6731.
[70] T. Abe, F. Taguchi, H. Imaya, F. Zhao, J. Zhang, M. Kaneko, *Polym. Adv. Technol.* **1998**, *9*, 559 – 562.
[71] F. Zhao, J. Zhang, T. Abe, D. Wohrle, M. Kaneko, *J. Mol. Catal. A* **1999**, *145*, 245 – 256.
[72] V. Fourmond, P.-A. Jacques, M. Fontecave, V. Artero, *Inorg. Chem.* **2010**, *49*, 10338 – 10347.
[73] M. T. M. Koper, E. Bouwman, *Angew. Chem.* **2010**, *122*, 3810 – 3812; *Angew. Chem. Int. Ed.* **2010**, *49*, 3723 – 3725.

[74] G. A. N. Felton, R. S. Glass, D. L. Lichtenberger, D. H. Evans, *Inorg. Chem.* **2006**, *45*, 9181 – 9184.
[75] Homoconjugation, a phenomenon in which the conjugate base is stabilized by hydrogen bond to the acid, further complicates the determination of the overpotential.
[76] C. P. Andrieux, C. Blocman, J. M. Dumasbouchiat, F. Mhalla, J. M. Saveant, *J. Electroanal. Chem.* **1980**, *113*, 19 – 40.
[77] M. Rudolph, *J. Electroanal. Chem.* **2003**, *543*, 23 – 39.
[78] M. Rudolph, *J. Electroanal. Chem.* **2004**, *571*, 289 – 307.
[79] M. Rudolph, *J. Electroanal. Chem.* **2003**, *558*, 171 – 176.
[80] M. Rudolph, *J. Comput. Chem.* **2005**, *26*, 619 – 632.
[81] M. Rudolph, *J. Comput. Chem.* **2005**, *26*, 633 – 641.
[82] M. Rudolph, *J. Comput. Chem.* **2005**, *26*, 1193 – 1204.
[83] Linearity is generally lost for higher concentrations of acid, for which diffusion of the substrate is no longer limiting.
[84] A. Le Goff, V. Artero, B. Jousselme, P. D. Tran, N. Guillet, R. Metaye, A. Fihri, S. Palacin, M. Fontecave, *Science* **2009**, *326*, 1384 – 1387.
[85] P. D. Tran, A. Le Goff, J. Heidkamp, B. Jousselme, N. Guillet, S. Palacin, H. Dau, M. Fontecave, V. Artero, *Angew. Chem.* **2011**, *123*, 1407 – 1410; *Angew. Chem. Int. Ed.* **2011**, *50*, 1371 – 1374.
[86] G. N. Schrauzer, R. J. Holland, *J. Am. Chem. Soc.* **1971**, *93*, 1505 – 1506.
[87] L. J. L. Haller, E. Mas-Marza, A. Moreno, J. P. Lowe, S. A. Macgregor, M. F. Mahon, P. S. Pregosin, M. K. Whittlesey, *J. Am. Chem. Soc.* **2009**, *131*, 9618 – 9619.
[88] A. J. M. Caffyn, S. G. Feng, A. Dierdorf, A. S. Gamble, P. A. Eldredge, M. R. Vossen, P. S. White, J. L. Templeton, *Organometallics* **1991**, *10*, 2842 – 2848.
[89] J. S. Figueroa, C. C. Cummins, *J. Am. Chem. Soc.* **2003**, *125*, 4020 – 4021.
[90] E. Szajna-Fuller, A. Bakac, *Eur. J. Inorg. Chem.* **2010**, 2488 – 2494.
[91] A. M. Tait, M. Z. Hoffman, E. Hayon, *J. Am. Chem. Soc.* **1976**, *98*, 86 – 93.
[92] E. Fujita, J. F. Wishart, R. van Eldik, *Inorg. Chem.* **2002**, *41*, 1579 – 1583.
[93] A. M. Bond, G. A. Lawrance, P. A. Lay, A. M. Sargeson, *Inorg. Chem.* **1983**, *22*, 2010 – 2021.
[94] The process is only observed at very negative potentials and is rapidly followed by reduction to the Co^0 state in an irreversible two-electron process.
[95] T. H. Chao, J. H. Espenson, *J. Am. Chem. Soc.* **1978**, *100*, 129 – 133.
[96] K. Izutsu, *Acid-Base Dissociation Constants in Dipolar Aprotic Solvents*, Blackwell Scientific, Oxford, UK, **1990**.
[97] The calculation for the heterolytic pathway can only be carried out if the cycle involves two consecutive protonation reactions that are combined to form the so-called H_2 evolution step.
[98] I. Bhugun, D. Lexa, J. M. Saveant, *J. Am. Chem. Soc.* **1996**, *118*, 3982 – 3983.
[99] Weak acids, such as Et_3NH^+ in CH_3CN that are unable to protonate Co^I, can protonate "Co^0"; H_2 evolution can then be catalyzed by the formation of a Co^{II} hydride species.
[100] A. Fihri, V. Artero, M. Razavet, C. Baffert, W. Leibl, M. Fontecave, *Angew. Chem.* **2008**, *120*, 574 – 577; *Angew. Chem. Int. Ed.* **2008**, *47*, 564 – 567.
[101] J. L. Dempsey, J. R. Winkler, H. B. Gray, *J. Am. Chem. Soc.* **2010**, *132*, 16774 – 16776.
[102] In that case, there is a large excess of Co^I relative to protons.
[103] J. P. Collman, Y. Y. Ha, P. S. Wagenknecht, M. A. Lopez, R. Guilard, *J. Am. Chem. Soc.* **1993**, *115*, 9080 – 9088.
[104] P. J. Toscano, T. F. Swider, L. G. Marzilli, N. Brescianipahor, L. Randaccio, *Inorg. Chem.* **1983**, *22*, 3416 – 3421.
[105] M. Fontecave, V. Artero, *C. R. Chim.* **2011**, *14*, 362 – 371.
[106] C. J. Curtis, A. Miedaner, R. Ciancanelli, W. W. Ellis, B. C. Noll, M. Rakowski DuBois, D. L. DuBois, *Inorg. Chem.* **2003**, *42*, 216 – 227.
[107] A. D. Wilson, R. H. Newell, M. J. McNevin, J. T. Muckerman, M. Rakowski DuBois, D. L. DuBois, *J. Am. Chem. Soc.* **2006**, *128*, 358 – 366.
[108] In that case, protonation of the ligand occurs before reduction at the metal and results in rapid elimination of the ligand from the cobalt coordination sphere.
[109] K. A. Vincent, A. Parkin, F. A. Armstrong, *Chem. Rev.* **2007**, *107*, 4366 – 4413.
[110] M. Wang, Y. Na, M. Gorlov, L. C. Sun, *Dalton Trans.* **2009**, 6458 – 6467.
[111] S. Matsuoka, K. Yamamoto, T. Ogata, M. Kusaba, N. Nakashima, E. Fujita, S. Yanagida, *J. Am. Chem. Soc.* **1993**, *115*, 601 – 609.
[112] T. Ogata, Y. Yamamoto, Y. Wada, K. Murakoshi, M. Kusaba, N. Nakashima, A. Ishida, S. Takamuku, S. Yanagida, *J. Phys. Chem.* **1995**, *99*, 11916 – 11922.
[113] J. Grodkowski, P. Neta, *J. Phys. Chem. A* **2000**, *104*, 1848 – 1853.
[114] T. Dhanasekaran, J. Grodkowski, P. Neta, P. Hambright, E. Fujita, *J. Phys. Chem. A* **1999**, *103*, 7742 – 7748.
[115] J. M. Lehn, R. Ziessel, *Proc. Natl. Acad. Sci. USA* **1982**, *79*, 701 – 704.
[116] P. W. Du, J. Schneider, G. G. Luo, W. W. Brennessel, R. Eisenberg, *Inorg. Chem.* **2009**, *48*, 8646.
[117] P. W. Du, J. Schneider, G. G. Luo, W. W. Brennessel, R. Eisenberg, *Inorg. Chem.* **2009**, *48*, 4952 – 4962.
[118] M. Kirch, J. M. Lehn, J. P. Sauvage, *Helv. Chim. Acta* **1979**, *62*, 1345 – 1384.
[119] S. F. Chan, M. Chou, C. Creutz, T. Matsubara, N. Sutin, *J. Am. Chem. Soc.* **1981**, *103*, 369 – 379.
[120] B. Probst, A. Rodenberg, M. Guttentag, P. Hamm, R. Alberto, *Inorg. Chem.* **2010**, *49*, 6453 – 6460.
[121] J. M. Lehn, J. P. Sauvage, *New J. Chem.* **1977**, *1*, 449 – 451.
[122] A. Moradpour, E. Amouyal, P. Keller, H. Kagan, *New J. Chem.* **1978**, *2*, 547 – 549.
[123] S. M. Feldt, E. A. Gibson, E. Gabrielsson, L. Sun, G. Boschloo, A. Hagfeldt, *J. Am. Chem. Soc.* **2010**, *132*, 16714 – 16724.
[124] I. I. Creaser, L. R. Gahan, R. J. Geue, A. Launikonis, P. A. Lay, J. D. Lydon, M. G. Mccarthy, A. W. H. Mau, A. M. Sargeson, W. H. F. Sasse, *Inorg. Chem.* **1985**, *24*, 2671 – 2680.
[125] P. A. Lay, A. W. H. Mau, W. H. F. Sasse, I. I. Creaser, L. R. Gahan, A. M. Sargeson, *Inorg. Chem.* **1983**, *22*, 2347 – 2349.
[126] R. Ziessel, J. Hawecker, J. M. Lehn, *Helv. Chim. Acta* **1986**, *69*, 1065 – 1084.
[127] C. V. Krishnan, N. Sutin, *J. Am. Chem. Soc.* **1981**, *103*, 2141 – 2142.
[128] C. V. Krishnan, C. Creutz, D. Mahajan, H. A. Schwarz, N. Sutin, *Isr. J. Chem.* **1982**, *22*, 98 – 106.
[129] C. Konigstein, R. Bauer, *Int. J. Hydrogen Energy* **1997**, *22*, 471 – 474.
[130] G. M. Brown, B. S. Brunschwig, C. Creutz, J. F. Endicott, N. Sutin, *J. Am. Chem. Soc.* **1979**, *101*, 1298 – 1300.
[131] J. Hawecker, J. M. Lehn, R. Ziessel, *New J. Chem.* **1983**, *7*, 271 – 277.
[132] $[Co(CN)_5(H_2O)]^{3-}$ in combination with a photosensitizer was also used for the light-driven H_2 evolution from alcohols, which were used as sacrificial electron donors: M. B. Rozenkevich, J. A. Sakharovsky, *Int. J. Hydrogen Energy* **1989**, *14*, 431 – 436.
[133] J. I. Goldsmith, W. R. Hudson, M. S. Lowry, T. H. Anderson, S. Bernhard, *J. Am. Chem. Soc.* **2005**, *127*, 7502 – 7510.
[134] J. L. Dempsey, B. S. Brunschwig, J. R. Winkler, H. B. Gray, *Acc. Chem. Res.* **2009**, *42*, 1995 – 2004.
[135] A. Fihri, V. Artero, A. Pereira, M. Fontecave, *Dalton Trans.* **2008**, 5567 – 5569.

[136] P. Zhang, M. Wang, J. Dong, X. Li, F. Wang, L. Wu, L. Sun, *J. Phys. Chem. C* **2010**, *114*, 15868 – 15874.
[137] P. Zhang, M. Chavarot-Kerlidou, P.-A. Jacques, M. Wang, L. Sun, M. Fontecave, V. Artero, unpublished results.
[138] B. Probst, C. Kolano, P. Hamm, R. Alberto, *Inorg. Chem.* **2009**, *48*, 1836 – 1843.
[139] P. W. Du, K. Knowles, R. Eisenberg, *J. Am. Chem. Soc.* **2008**, *130*, 12576 – 12577.
[140] X. Wang, S. Goeb, Z. Ji, N. A. Pogulaichenko, F. N. Castellano, *Inorg. Chem.* **2011**, *50*, 705 – 707.
[141] T. Lazarides, T. McCormick, P. W. Du, G. G. Luo, B. Lindley, R. Eisenberg, *J. Am. Chem. Soc.* **2009**, *131*, 9192 – 9194.
[142] T. M. McCormick, B. D. Calitree, A. Orchard, N. D. Kraut, F. V. Bright, M. R. Detty, R. Eisenberg, *J. Am. Chem. Soc.* **2010**, *132*, 15480 – 15483.
[143] C. Li, M. Wang, J. X. Pan, P. Zhang, R. Zhang, L. C. Sun, *J. Organomet. Chem.* **2009**, *694*, 2814 – 2819.
[144] H. Ozawa, M. A. Haga, K. Sakai, *J. Am. Chem. Soc.* **2006**, *128*, 4926 – 4927.
[145] H. Ozawa, K. Sakai, *Chem. Lett.* **2007**, *36*, 920 – 921.
[146] S. Rau, B. Schäfer, D. Gleich, E. Anders, M. Rudolph, M. Friedrich, H. Görls, W. Henry, J. G. Vos, *Angew. Chem.* **2006**, *118*, 6361 – 6364; *Angew. Chem. Int. Ed.* **2006**, *45*, 6215 – 6218.
[147] S. Tschierlei, M. Karnahl, M. Presselt, B. Dietzek, J. Guthmuller, L. Gonzalez, M. Schmitt, S. Rau, J. Popp, *Angew. Chem.* **2010**, *122*, 4073 – 4076; *Angew. Chem. Int. Ed.* **2010**, *49*, 3981 – 3984.
[148] M. Elvington, J. Brown, S. M. Arachchige, K. J. Brewer, *J. Am. Chem. Soc.* **2007**, *129*, 10644 – 10645.
[149] A. F. Heyduk, D. G. Nocera, *Science* **2001**, *293*, 1639 – 1641.
[150] S. Jasimuddin, T. Yamada, K. Fukuju, J. Otsuki, K. Sakai, *Chem. Commun.* **2010**, *39*, 8466 – 8468.
[151] P. Zhang, M. Wang, C. Li, X. Li, J. Dong, L. Sun, *Chem. Commun.* **2010**, *46*, 8806 – 8809.
[152] K. L. Mulfort, D. M. Tiede, *J. Phys. Chem. B* **2010**, *114*, 14572 – 14581.
[153] F. Lakadamyali, E. Reisner, *Chem. Commun.* **2011**, *47*, 1695 – 1697.
[154] U. Kölle, *New J. Chem.* **1992**, *16*, 157 – 169.
[155] P. Lei, M. Hedlund, R. Lomoth, H. Rensmo, O. Johansson, L. Hammarström, *J. Am. Chem. Soc.* **2008**, *130*, 26 – 27.
[156] A similar description of the excited and oxidized states holds for the other iridium and rhenium diimine photosensitizers discussed in this section.
[157] A. Juris, V. Balzani, F. Barigelletti, S. Campagna, P. Belser, A. Vonzelewsky, *Coord. Chem. Rev.* **1988**, *84*, 85 – 277.
[158] This contrasts with electrocatalytic studies in which the interfacial electron transfer at the electrode is generally not considered as the kinetic bottleneck for H_2 evolution.
[159] P. D. Tran, V. Artero, M. Fontecave, *Energy Environ. Sci.* **2010**, *3*, 727 – 747.
[160] R. M. Kellett, T. G. Spiro, *Inorg. Chem.* **1985**, *24*, 2378 – 2382.
[161] A. B. Soto, E. M. Arce, M. Palomar-Pardavé, I. Gonzalez, *Electrochim. Acta* **1996**, *41*, 2647 – 2655.
[162] S. Trasatti, *Electrochim. Acta* **1984**, *29*, 1503 – 1512.
[163] M. R. Tarasevich, B. N. Efremov, *Electrodes of Conductive Metal Oxides* (Ed.: S. Trasatti), Elsevier, Amsterdam, **1980**, chap. 5, and references therein.
[164] S. D. Tilley, M. Cornuz, K. Sivula, M. Grätzel, *Angew. Chem.* **2010**, *122*, 6549 – 6552; *Angew. Chem. Int. Ed.* **2010**, *49*, 6405 – 6408.
[165] W. J. Youngblood, S. H. A. Lee, Y. Kobayashi, E. A. Hernandez-Pagan, P. G. Hoertz, T. A. Moore, A. L. Moore, D. Gust, T. E. Mallouk, *J. Am. Chem. Soc.* **2009**, *131*, 926 – 927.
[166] Nickel oxide is classically the basis of active anodes used for alkaline electrolysis with a similar overpotential requirement.
[167] H. Dau, I. Zaharieva, *Acc. Chem. Res.* **2009**, *42*, 1861 – 1870.
[168] L. Li, L. L. Duan, Y. H. Xu, M. Gorlov, A. Hagfeldt, L. C. Sun, *Chem. Commun.* **2010**, *46*, 7307 – 7309.
[169] S. W. Gersten, G. J. Samuels, T. J. Meyer, *J. Am. Chem. Soc.* **1982**, *104*, 4029 – 4030.
[170] R. Cao, H. Y. Ma, Y. V. Geletii, K. I. Hardcastle, C. L. Hill, *Inorg. Chem.* **2009**, *48*, 5596 – 5598.
[171] Y. V. Geletii, Z. Q. Huang, Y. Hou, D. G. Musaev, T. Q. Lian, C. L. Hill, *J. Am. Chem. Soc.* **2009**, *131*, 7522 – 7523.
[172] A. A. Noyes, T. J. Deahl, *J. Am. Chem. Soc.* **1937**, *59*, 1337 – 1344.
[173] J. Veprek-Siska, V. Ettel, *J. Inorg. Nucl. Chem.* **1969**, *31*, 789 – 798.
[174] J. Veprek-Siska, V. Ettel, *Chem. Ind.* **1967**, 548 – 549.
[175] M. Anbar, I. Pecht, *Trans. Faraday Soc.* **1968**, *64*, 744 – 750.
[176] V. Y. Shafirovich, N. K. Khannanov, V. V. Strelets, *New J. Chem.* **1980**, *4*, 81 – 84.
[177] M. Anbar, I. Pecht, *J. Am. Chem. Soc.* **1967**, *89*, 2553 – 2556.
[178] V. Y. Shafirovich, V. V. Strelets, *New J. Chem.* **1978**, *2*, 199 – 201.
[179] B. S. Brunschwig, M. H. Chou, C. Creutz, P. Ghosh, N. Sutin, *J. Am. Chem. Soc.* **1983**, *105*, 4832 – 4833.
[180] Q. S. Yin, J. M. Tan, C. Besson, Y. V. Geletii, D. G. Musaev, A. E. Kuznetsov, Z. Luo, K. I. Hardcastle, C. L. Hill, *Science* **2010**, *328*, 342 – 345.
[181] T. J. R. Weakley, H. T. Evans, J. S. Showell, G. F. Tourne, C. M. Tourne, *J. Chem. Soc. Chem. Commun.* **1973**, 139 – 140.
[182] R. Vittal, H. Gomathi, G. P. Rao, *J. Electroanal. Chem.* **2001**, *497*, 47 – 54.
[183] T. Schmidt, H. Wendt, *Electrochim. Acta* **1994**, *39*, 1763 – 1767.
[184] P. Benson, G. W. D. Briggs, W. F. K. Wynne-Jones, *Electrochim. Acta* **1964**, *9*, 275 – 280.
[185] P. Benson, G. W. D. Briggs, W. F. K. Wynne-Jones, *Electrochim. Acta* **1964**, *9*, 281 – 288.
[186] O. Suzuki, M. Takahashi, T. Fukunaga, J. Kuboyama, US Patent 3,399,966, **1968**.
[187] Y. W. D. Chen, R. N. Noufi, *J. Electrochem. Soc.* **1984**, *131*, 1447 – 1451.
[188] C. Q. Cui, S. P. Jiang, A. C. C. Tseung, *J. Electrochem. Soc.* **1992**, *139*, 1535 – 1544.
[189] C. Q. Cui, S. P. Jiang, A. C. C. Tseung, *J. Electrochem. Soc.* **1992**, *139*, 1276 – 1282.
[190] C. Q. Cui, S. P. Jiang, A. C. C. Tseung, *J. Electrochem. Soc.* **1992**, *139*, 60 – 66.
[191] S. P. Jiang, W. R. Ashton, A. C. C. Tseung, *J. Catal.* **1991**, *131*, 88 – 93.
[192] S. P. Jiang, Y. Z. Chen, J. K. You, T. X. Chen, A. C. C. Tseung, *J. Electrochem. Soc.* **1990**, *137*, 3374 – 3380.
[193] S. P. Jiang, C. Q. Cui, A. C. C. Tseung, *J. Electrochem. Soc.* **1991**, *138*, 3599 – 3605.
[194] S. P. Jiang, A. C. C. Tseung, *J. Electrochem. Soc.* **1990**, *137*, 3381 – 3386.
[195] S. P. Jiang, A. C. C. Tseung, *J. Electrochem. Soc.* **1990**, *137*, 3387 – 3393.
[196] S. P. Jiang, A. C. C. Tseung, *J. Electrochem. Soc.* **1991**, *138*, 1216 – 1222.
[197] Y. H. Ni, X. W. Ge, Z. C. Zhang, H. R. Liu, Z. L. Zhu, Q. Ye, *Mater. Res. Bull.* **2001**, *36*, 2383 – 2387.
[198] W. L. Guo, Y. F. E, L. Gao, L. Z. Fan, S. H. Yang, *Chem. Commun.* **2010**, *46*, 1290 – 1292.
[199] M. E. G. Lyons, M. P. Brandon, *Int. J. Electrochem. Sci.* **2008**, *3*, 1425 – 1462.
[200] J. Tyczkowski, R. Kapica, J. Lojewska, *Thin Solid Films* **2007**, *515*, 6590 – 6595.
[201] L. C. Schumacher, I. B. Holzhueter, I. R. Hill, M. J. Dignam, *Electrochim. Acta* **1990**, *35*, 975 – 984.
[202] A. J. Esswein, M. J. McMurdo, P. N. Ross, A. T. Bell, T. D. Tilley, *J. Phys. Chem. C* **2009**, *113*, 15068 – 15072.

[203] R. N. Singh, D. Mishra, Anindita, A. S. K. Sinha, A. Singh, *Electrochem. Commun.* **2007**, *9*, 1369 – 1373.
[204] F. Jiao, H. Frei, *Energy Environ. Sci.* **2010**, *3*, 1018 – 1027.
[205] M. E. G. Lyons, M. P. Brandon, *J. Electroanal. Chem.* **2010**, *641*, 119 – 130.
[206] M. W. Kanan, D. G. Nocera, *Science* **2008**, *321*, 1072 – 1075.
[207] Y. Surendranath, M. Dinca, D. G. Nocera, *J. Am. Chem. Soc.* **2009**, *131*, 2615 – 2620.
[208] M. W. Kanan, J. Yano, Y. Surendranath, M. Dinca, V. K. Yachandra, D. G. Nocera, *J. Am. Chem. Soc.* **2010**, *132*, 13692 – 13701.
[209] M. Risch, V. Khare, I. Zaharieva, L. Gerencser, P. Chernev, H. Dau, *J. Am. Chem. Soc.* **2009**, *131*, 6936 – 6937.
[210] H. Dau, C. Limberg, T. Reier, M. Risch, S. Roggan, P. Strasser, *ChemCatChem* **2010**, *2*, 724 – 761.
[211] E. R. Young, D. G. Nocera, V. Bulovic, *Energy Environ. Sci.* **2010**, *3*, 1726 – 1728.
[212] A. J. Esswein, Y. Surendranath, S. Y. Reece, D. G. Nocera, *Energy Environ. Sci.* **2011**, *4*, 499 – 504.
[213] Y. Surendranath, M. W. Kanan, D. G. Nocera, *J. Am. Chem. Soc.* **2010**, *132*, 16501 – 16509.
[214] J. G. McAlpin, Y. Surendranath, M. Dinca, T. A. Stich, S. A. Stoian, W. H. Casey, D. G. Nocera, R. D. Britt, *J. Am. Chem. Soc.* **2010**, *132*, 6882 – 6883.
[215] D. A. Lutterman, Y. Surendranath, D. G. Nocera, *J. Am. Chem. Soc.* **2009**, *131*, 3838 – 3839.
[216] A similar repair mechanism for cobalt oxide films in the presence of phosphate ions was observed in 1950: S. E. S. El Wakkad, A. Hickling, *Trans. Faraday Soc.* **1950**, *46*, 820.
[217] J. B. Gerken, E. C. Landis, R. J. Hamers, S. S. Stahl, *ChemSusChem* **2010**, *3*, 1176 – 1179.
[218] The same is true for other anions, such as borate and methylphosphonate.[213]
[219] A. Harriman, G. Porter, P. Walters, *J. Chem. Soc. Faraday Trans. 2* **1981**, *77*, 2373 – 2383.
[220] D. Shevchenko, M. F. Anderlund, A. Thapper, S. Styring, *Energy Environ. Sci.* **2011**, *4*, 1284 – 1287.
[221] A. Harriman, I. J. Pickering, J. M. Thomas, P. A. Christensen, *J. Chem. Soc. Faraday Trans. 1* **1988**, *84*, 2795 – 2806.
[222] F. Jiao, H. Frei, *Angew. Chem.* **2009**, *121*, 1873 – 1876; *Angew. Chem. Int. Ed.* **2009**, *48*, 1841 – 1844.
[223] Z. Huang, Z. Luo, Y. V. Geletii, J. W. Vickers, Q. Yin, D. Wu, Y. Hou, Y. Ding, J. Song, D. G. Musaev, C. L. Hill, T. Lian, *J. Am. Chem. Soc.* **2011**, *133*, 2068 – 2071.
[224] C. Baffert, S. Romain, A. Richardot, J. C. Lepretre, B. Lefebvre, A. Deronzier, M. N. Collomb, *J. Am. Chem. Soc.* **2005**, *127*, 13694 – 13704.
[225] K. Nagashima, M. Inoue, H. Namiki, *Electrochemistry* **2000**, *68*, 651 – 652.
[226] T. Abe, K. Nagai, S. Kabutomori, M. Kaneko, A. Tajiri, T. Noritnatsit, *Angew. Chem.* **2006**, *118*, 2844 – 2847; *Angew. Chem. Int. Ed.* **2006**, *45*, 2778 – 2781.
[227] A. Kay, I. Cesar, M. Grätzel, *J. Am. Chem. Soc.* **2006**, *128*, 15714 – 15721.
[228] D. K. Zhong, J. W. Sun, H. Inumaru, D. R. Gamelin, *J. Am. Chem. Soc.* **2009**, *131*, 6086 – 6087.
[229] D. K. Zhong, D. R. Gamelin, *J. Am. Chem. Soc.* **2010**, *132*, 4202 – 4207.
[230] E. M. P. Steinmiller, K. S. Choi, *Proc. Natl. Acad. Sci. USA* **2009**, *106*, 20633 – 20636.
[231] D. G. Nocera, M. W. Kanan, T. A. Moore, Y. Surendranath, S. Y. Reece, A. J. Esswein, WO 042197A1, **2010**.
[232] M. Grätzel, *Nature* **2001**, *414*, 338 – 344.
[233] N. D. McDaniel, S. Bernhard, *Dalton Trans.* **2010**, *39*, 10021 – 10030.
[234] A. J. Bard, *J. Am. Chem. Soc.* **2010**, *132*, 7559 – 7567.
[235] The first reduction step of $S_2O_8^{2-}$, yielding SO_4^{2-} and the radical species $SO_4^{\bullet-}$, occurs at a quite mild potential of 0.6 V vs NHE: R. Memming, *J. Electrochem. Soc.* **1969**, *116*, 785 – 790.
[236] Since this Review was accepted for publication, a number of reports have appeared regarding cobalt-based catalytic and photocatalytic molecular systems for both hydrogen evolution and water oxidation. The molecular nature of the catalyst has also been questioned in the case of water-oxidizing systems. For example, in the case of an immobilized manganese-based catalyst, it has been confirmed that the active species for water oxidation is a metal oxide: R. K. Hocking, R. Brimblecombe, L.-Y. Chang, A. Singh, M. H. Cheah, C. Glover, W. H. Casey, L. Spiccia, *Nature Chemistry*, **2011**, *3*, 461 – 466. Similar observations have been made for molecular cobalt complexes that form an amorphous cobalt oxide film under catalytic conditions for water oxidation in a potassium phosphate buffer. J. Luo, N. P. Rath, L. M. Mirica, *Inorg. Chem.* **2011**, DOI: 10.1021/ic201031s.

